JNCASR

March 2014

Preliminary Studies on *Plasmodium falciparum* Adenosine 5′Monophosphate Deaminase

A thesis submitted for the partial fulfilment of the degree of

Master of Science

As a part of Integrated Ph.D. Programme

(Biological Sciences)

By

Lakshmeesha K N

Molecular Biology and Genetics Unit

Jawaharlal Nehru Centre for Advanced Scientific Research

(A Deemed University)

Jakkur, Bangalore - 560064

Declaration

I hereby declare that this thesis entitled, **"Preliminary Studies on *Plasmodium falciparum* Adenosine 5′ Monophosphate Deaminase"** is an authentic record of research work, which has been carried by me under the supervision of Prof. Hemalatha Balaram at the Molecular Biology and Genetics Unit, Jawaharlal Nehru Centre for Advanced Scientific Research, Bangalore, India and this work has not been submitted elsewhere for the award of any other degree.

In keeping with the general practice of reporting scientific observations, due acknowledgements have been made wherever the work described has been based on the findings of other investigators. Any omission, which might have occurred by oversight or misjudgement, is regretted.

JNCASR, Bangalore **(Lakshmeesha K N)**

March 2014.

Molecular Biology and Genetics Unit
Jawaharlal Nehru Centre for Advanced Scientific Research
Jakkur, Bengaluru-560 064, India

Hemalatha Balaram, Ph.D.

Professor

Certificate

This is to certify that the work described in this thesis entitled **"Preliminary Studies on *Plasmodium falciparum* Adenosine 5′ Monophosphate Deaminase"** is the result of investigations carried out by Mr. Lakshmeesha K N in the Molecular Biology and Genetics Unit, Jawaharlal Nehru Centre for Advanced Scientific Research, Bangalore, India under my supervision, and that the results presented in this thesis have not been previously formed the basis for the award of any other diploma, degree or fellowship.

JNCASR, Bangalore **(Hemalatha Balaram)**

March 2014.

♦Telephone: 91-80-22082812 ♦Telefax: 91-80-22082766 ♦Email: hb@jncasr.ac.in

Acknowledgements

I hereby express my heartfelt regards to Prof. Hemalatha Balaram, for providing me a valuable opportunity to work in her lab and also for her guidance without which this project would have been a difficult venture.

I would like to thank all the faculty of MBGU, whose course work helped me immensely in understanding some of the fundamental concepts in biology.

I am highly indebted to Dr.Ramesh (our beloved Ramesh Sir) who taught us not only science, but also discipline and ethics in science, during our practical course.

I would like to thank Mr. Sourav Roy and Dr. Vasudeva S P, for mentoring and teaching me during my lab rotation.

Also, I would like to thank all my lab mates Mr. Sanjeev Kumar, Mr. Vijay Jayaraman, Mr. Arpit Prakshkumar Shukla, Mr. Santosh, Ms. Lakshmi Prasoona Thota, Mr. Umesh T G, Ms. Jyothirmayi Kunala, Ms. Sonia Kulkarni, Ms. Vidhi Pareek, Ms Debarati Bandyopadhyaya, Ms. Keerthana, Ms. Arpitha Sooryavamshi, Ms. Meenakshi P, Ms. Aparna V Dongre, Mr. Manu Sathya and Mr. Balakrishna, for providing a great working environment and for their valuable suggestions.

I would like to thank Dr. Ravi Manjithaya, in whose lab I did my second lab rotation. Part of the work in my thesis was possible because of the skills I learned in his lab.

I would like to thank all Autophagy lab members; especially Mr. Suresh S N and Mr. Shashank Rai; for their extensive help.

I would like to thank Anita mam, Suma mam and Dr. Prakash for their help and support.

I would like to thank my family & friends in JNC and University of Mysore for their love and support.

I would like to thank JNCASR for providing such a conducive environment to work.

- ***Lakshmeesha K N***

List of abbreviations

Ade	**Adenine**
ADP	**Adenosine diphosphate**
AEC	**Adenylate energy charge**
AK	**Adenosine kinase**
AMP	**Adenosine 5′monophosphate**
AMPD	**AMP deaminase**
APRT	**Adenine phosphoribosyl transferase**
ATP	**Adenosine triphosphate**
DTT	**Di-thio threitol**
GMP	**Guanosine 5′monophosphate**
GdmCl	**Guanidinium Hydrochloride**
GTP	**Guanosine triphosphate**
HGPRT	**Hypoxanthine guanine phosphoribosyl transferase**
HGXPRT	**Hypoxanthine guanine xanthine phosphoribosyl transferase**
IMP	**Inosine 5′monophosphate**
IPTG	**Isopropyl thio – β – D – galactopyranoside**
OD	**Optical density**
OMP	**Orotate 5′monophosphate**
OMPD	**OMP decarboxylase**
OPRT	**Orotate phosphoribosyl transferase**
PRPP	**Phosphoribosyl pyrophosphate**
SAM	**S – adenosyl methionine**
SD	**Synthetically defined**
SDS	**Sodium dodecyl sulphate**
UPRT	**Uracil phosphoribosyl transferase**
XMP	**Xanthine 5′monophosphate**
YPD	**Yeast extract peptone dextrose**

Table of contents

Chapter 1	**• Introduction**
Chapter 2	• Expression of PfAMPD in *E. coli* and yeast
Chapter 3	• Localization studies in *P. falciparum*
Chapter 4	• Complementation studies in AMPD knockout yeast strain

Chapter 1 – INTRODUCTION

1.1 Synopsis

The current study focuses on the preliminary characterisation of a purine nucleotide cycle enzyme, AMP deaminase (AMPD hereafter) from *Plasmodium falciparum*. Purine nucleotide cycle performs inter-conversion of IMP and AMP with the release of fumarate and ammonia as by-products, which also have physiological consequences. The pathway plays a chief role in maintaining adenylate energy charge ratio, which is critical for cell survival. Cloning, expression and preliminary characterization of the enzyme has been reported in this thesis.

1.2 Introduction to nucleotide metabolism

Apart from being building blocks of the genetic material, the bio-molecules which are also used as energy currency of the cell and cofactors for enzymes, are nucleotides. Hence nucleotide metabolism forms an integral part of intermediary metabolism. Purine and pyrimidine nucleotides can be synthesised by both *de novo* and salvage pathways [Figure 1]. *De novo* pathway involves synthesis of purine ribonucleotides starting from the substrate ribose 5′ phosphate, which is acted upon by various enzymes, in order to form IMP. This IMP can then be used as substrate for the synthesis of adenine nucleotides or guanine nucleotides. Pyrimidine nucleotides are synthesised starting from carbamoyl phosphate and result in UMP which is later converted to UTP or CTP. The salvage pathway employs phosphoribosyltransferases which catalyse transfer of phosphoribosyl moiety from PRPP to the free nitrogen base such as adenine, guanine, hypoxanthine, xanthine and uracil to yield respective mono nucleotides. Salvage pathway also involves nucleoside kinases which phosphorylate nucleosides to generate nucleotides.

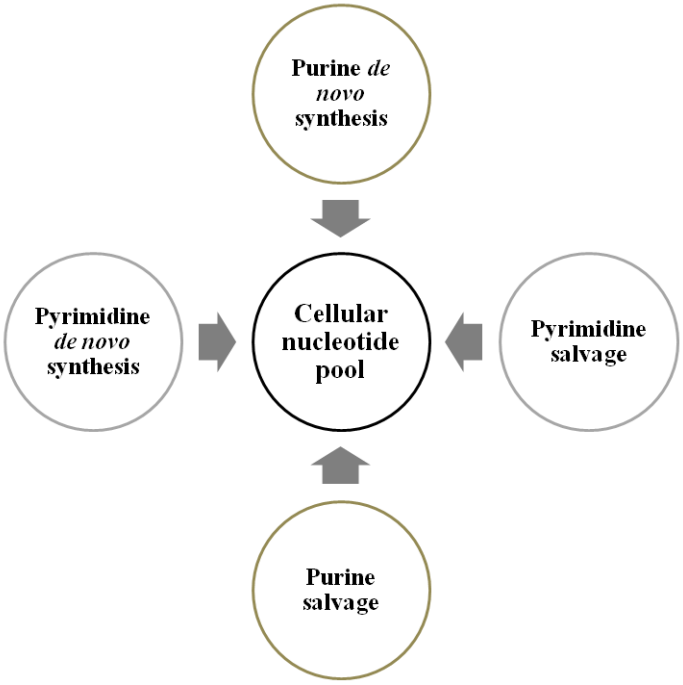

Figure 1.Schematic representation of different routes of nucleotide synthesis

1.3 Plasmodium nucleotide metabolism – 'a soft spot for drugs'

The protozoan parasite *Plasmodium falciparum* seems to become invincible for most of the anti – malarial agents available in the market. The parasite has been existing along with its host for millions of years and has evolved mechanisms to escape from the host immune system and develop resistance to anti malarial drugs. Nucleotide synthesis in the parasitic protozoan *P. falciparum* is characterised by the absence of *de novo* purine biosynthetic pathway and pyrimidine salvage pathway [Figure 2]. Hence the parasite is forced to salvage the purine bases from its host and generate its cellular purine nucleotide pool by salvage pathway enzymes. This feat is achieved predominantly by hypoxanthine guanine xanthine phosphoribosyltransferase which can act on hypoxanthine; guanine and xanthine to form IMP, GMP and XMP. The predominant nitrogen base that is salvaged is hypoxanthine and the IMP thus formed is used to synthesise AMP or GMP (*Downie et.al, 2008*). Though the parasite lacks the enzymes APRT and adenosine kinase, it has the ability to import AMP from the erythrocytes by nucleotide receptors present on parasite plasma membrane (*Cassera et al., 2008; Roth et al., 2013*). However it is not clear if this uptake of AMP is of any

significant magnitude. These properties of the parasites' metabolism make it a hot target for drugs which have potential use for anti malarial therapy.

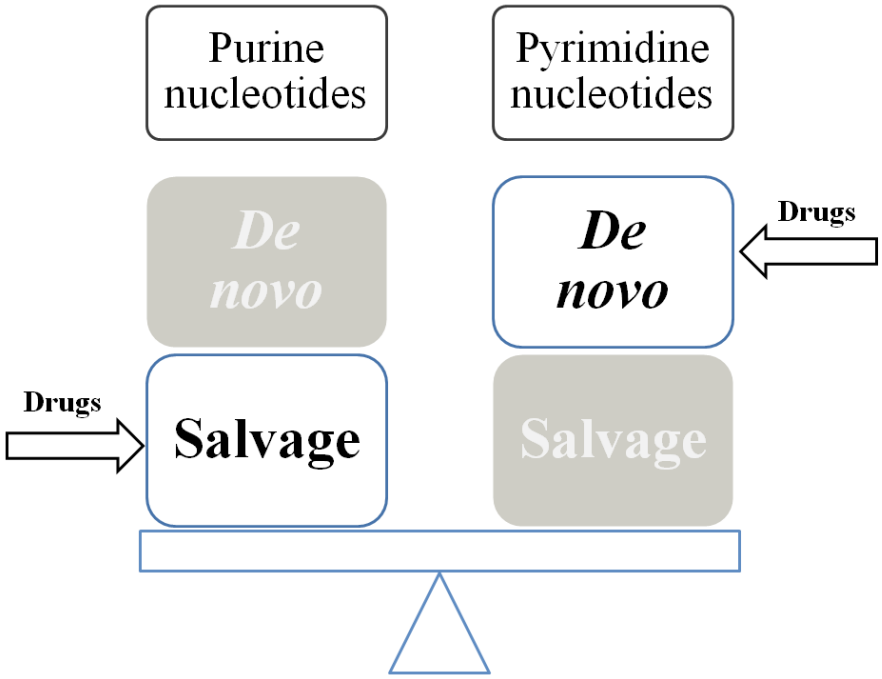

Figure 2.Schematic representation of nucleotide metabolism in P. falciparum, shaded pathways are absent, arrows indicate pathways that can be target for anti malarial drugs.

1.4 Purine nucleotide cycle and its role in 'adenylate energy charge' homeostasis

Purine nucleotide cycle is a branch pathway of the purine nucleotide biosynthetic pathway. It comprises of three enzymes namely adenylosuccinate synthetase, adenylosuccinate lyase and AMP deaminase. These three catalyse the inter-conversion of AMP and IMP [Figure 3]. IMP coming from either *de novo* or salvage pathway gets converted to succinyl AMP by the action of enzyme adenylosuccinate synthetase. Succinyl AMP gets hydrolysed to give AMP and fumarate. AMP gets deaminated back to IMP by AMP deaminase. The main products of the cycle are fumarate and ammonia. Fumarate is known to feed in to tricarboxylic acid cycle and hence performs the role of anapleurosis (*Jayaraman et al., 2011)*. Whereas in case of ammonia, there are two schools of thought; one claiming that ammonia is a metabolic waste and the other arguing that it will accept H^+ ions and act as a buffer system (*Lowenstein, 1972*).

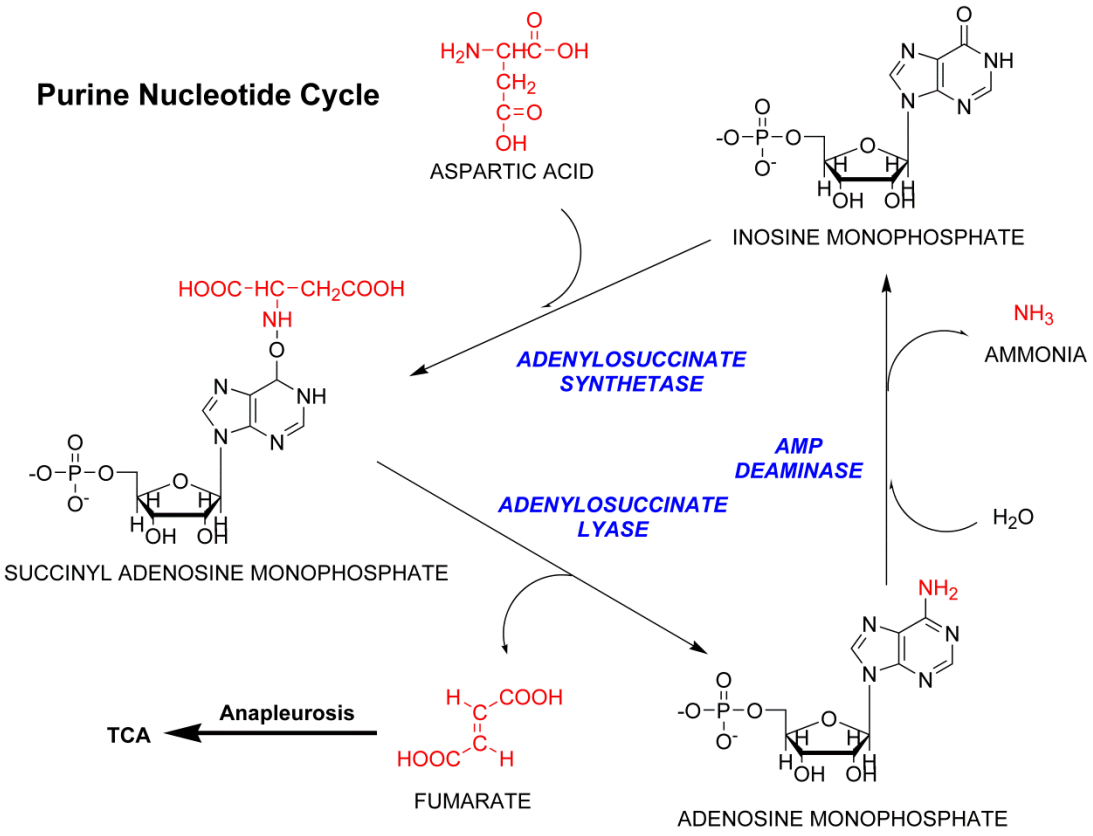

Figure 3.Purine nucleotide cycle – enzymes and metabolites involved

Another important role of purine nucleotide cycle is to maintain *'Adenylate Energy Charge'* (AEC) of the cell. AEC is a measure of the cell's adenylate pool, which can perform phosphorylation. It is basically an index representing the high energy phosphoanhydride bonds present in the adenylate pool of a cell. Its mathematical representation was given by Daniel E. Atkinson which is as follows:

$$AEC = \frac{[ATP] + 0.5[ADP]}{[ATP] + [ADP] + [AMP]}$$

The AEC of a cell is essentially a ratio of sum of molar concentration of ATP and half the molar concentration of ADP to the total adenylate pool (*Chapman et al., 1971*). This ratio is highly regulated and fluctuates within a narrow range. The values of AEC under different conditions are given in Table 1.

Table 1.AEC values of a prokaryotic cell under different conditions (Atkinson, 1971 and Bancroft, 1975)

Condition	AEC value
Actively metabolizing cells	0.85 (0.7 – 0.9)
Stationary growth	0.6
Senescent cells	0.5
Compromised viability	< 0.5

AEC value is affected by various aspects of ATP generating processes and ATP consuming processes. Apart from this purine nucleotide cycle pathway enzymes and adenylate kinase reaction are known to maintain AEC of a cell (*Chapman et al., 1973*). Anabolic and catabolic pathways have a direct impact on AEC as they are involved in either consumption of ATP or generation of ATP. But purine nucleotide cycle and adenylate kinase reaction regulate AEC in a more sophisticated manner, which is described below.

Purine nucleotide cycle can be divided in to two arms; an AMP generating arm and an AMP depleting arm. The former comprises of two enzymes adenylosuccinate synthetase (ADSS) and adenylosuccinate lyase (ASL) which convert IMP to AMP along with the generation of a fumarate molecule. The latter arm, which has a single enzyme AMP deaminase (AMPD), converts AMP back to IMP. Under conditions when AEC drops below optimum the ADSS-ASL arm is down regulated and AMPD arm is up-regulated. This, results in stalling of AMP production and conversion of existing AMP to IMP, thereby the AEC value will be restored to normal at an expense of net loss of the adenylate pool concentration. When there is an increase in AEC the ADSS-ASL arm generates AMP which gets accumulated, as there is a down regulation of AMPD; resulting in restoration of AEC to normal value (*Hellsten et al., 1999*). Extensive metabolite profiling experiments have given

substantial evidence validating this mechanism employed by cells to maintain AEC (*Kalsi et al., 2003; Lanaspa et al., 2012; Li et al., 2013*).

AMP deaminase is an interesting candidate as it can modulate AEC by being part of purine nucleotide cycle as well as by independently regulating the equilibrium of the adenylate kinase reaction [Figure 4].

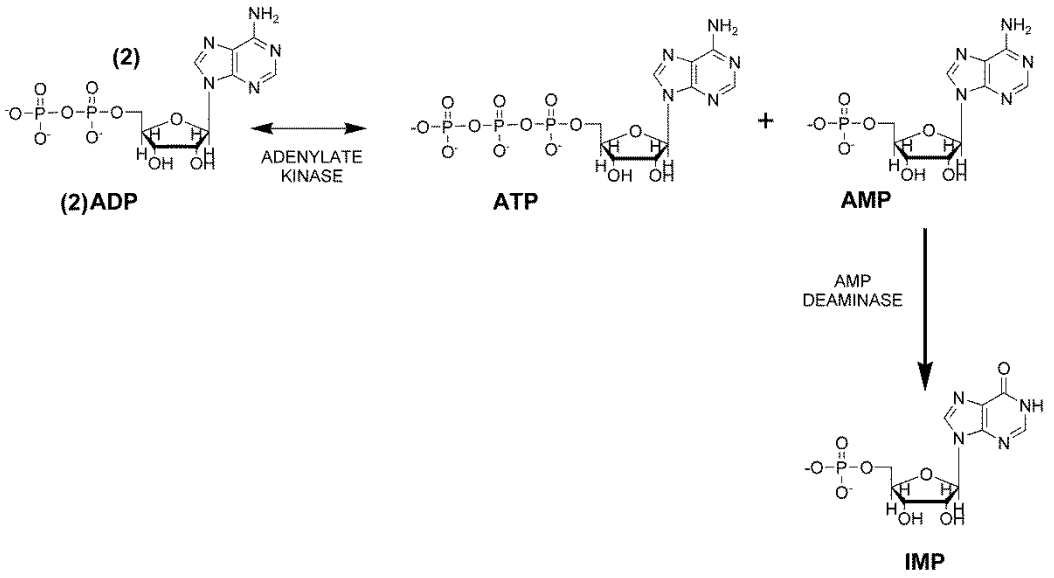

Figure 4.Reaction scheme of adenylate kinase and AMPD

Adenylate kinase catalyses the reversible reaction; where two ADP molecules are converted to one ATP and one AMP. This reaction maintains the three way equilibrium between ATP, ADP and AMP levels in a cell. The ATP generated will be utilized by energy consuming processes, while AMP gets deaminated to IMP by AMPD. When there is excessive ATP catabolism, the increased generation of ADP drives the adenylate kinase reaction towards right side of the reaction and helps in replenishing ATP pools partially. This reaction becomes very critical for tissues like skeletal muscle tissue, as the energy requirement is high. In conditions where AMPD is not operating (either due to a mutation in case of the genetic disorder, myoadenylate deaminase deficiency, or in case of a knock out cell where the gene has been deleted) AMP accumulation takes place and this exerts a feedback inhibition on the adenylate kinase reaction and shifts the reaction towards left. This leads to several

consequences; most prominent in the literature is the fatigue and muscle weakness reported in subjects suffering from myoadenylate deaminase deficiency, an autosomal recessive genetic disorder (*Hellsten et al., 1999; Isackson et al., 2005; Mineo et al., 1985, and Sabina et al., 1984).* Insufficient production of ATP and accumulation of AMP synergistically bring down the AEC of the cell in the absence of AMPD activity. Homeostasis of the AEC of a given cell is highly dependent on the flux through the two arms of purine nucleotide cycle as well as the adenylate kinase reaction which is in turn regulated by AMPD.

1.5 Introduction to Amidohydrolase super family of enzymes and their classification

AMP deaminase which plays a key role in maintenance of AEC belongs to amidohydrolase superfamily of enzymes. Amidohydrolase superfamily consists of members who share similarity in structure as well as in mechanism of action which involves metal assisted hydrolysis of an amide or ester bond at a carbon or phosphorous atom. The members of the family have either one or two divalent metal ion centres which are involved in catalytic mechanisms such as deamination, decarboxylation, dechlorination, dephosphorylation and isomerisation. The proteins belonging to this family have an α_8/β_8 TIM barrel structure, where most of the catalytic residues are clustered at the C – terminus. Structural characterization by X-Ray crystallography has revealed seven variations in this family based on the amino acid residues involved in the ligation of the metal ion. Divalent zinc is the predominantly found metal ion in this family, whereas there are examples containing zinc and nickel, zinc and iron or iron alone in the structure. Histidine, aspartate and glutamate residues from the beta strands are known to form complex with the metal centre (*Siebert and Raushel, 2005; Marotta et al., 2009 and Nam et al., 2005, Arbona, 2006*). Schematic representation of structure a member of amidohydrolase superfamily is shown in Figure 5.

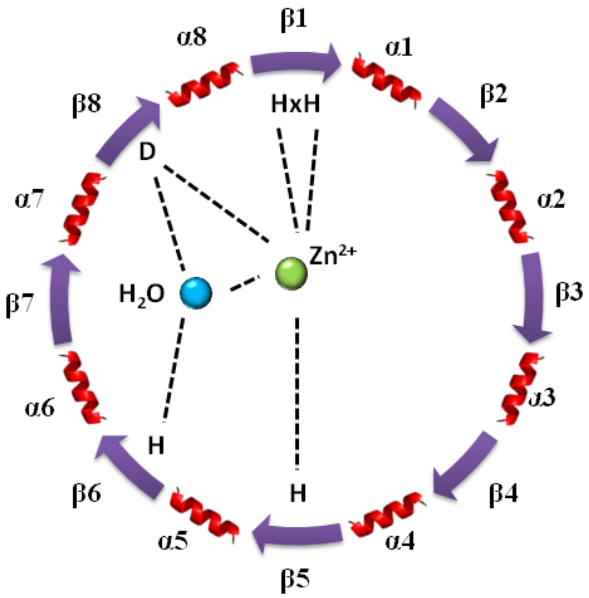

Figure 5.Schematic representation of α_8/β_8 TIM barrel structure of one sub class of amidohydrolase superfamily. AMP deaminase belongs to this class and shown are the residues from various β strands which co-ordinate with the metal ion.

Amidohydrolase family of proteins have members which catalyse diverse reactions such as phosphotriesterase, urease, dihydroorotase, isoaspartyl dipeptidase, D-hydantoinase, uronate isomerase, D-amino acid deacetylase. Also *Enzyme Function Initiative* reports 730 members in this family. The conserved structure and catalytic mechanism reflects intelligent evolution of this family from an ancestral enzyme.

1.6 AMP deaminase – sequence, structure, mechanism and function

AMP deaminases are proteins with huge sequence diversity. AMPD isolated from various sources like fungi, plants and mammalian tissues have diverse N terminus sequence but a conserved C terminus comprising the catalytic residues. The literature available so far have reported biochemical characterization of N terminal truncated forms of AMPD as this region is known to be highly disordered with high propensity for proteolytic degradation (*Jurken et al., 1995*). Analysis of the sequences of various AMPD has revealed diversity in protein length as well. Figure 6 shows number of amino acid residues in AMPD protein across species.

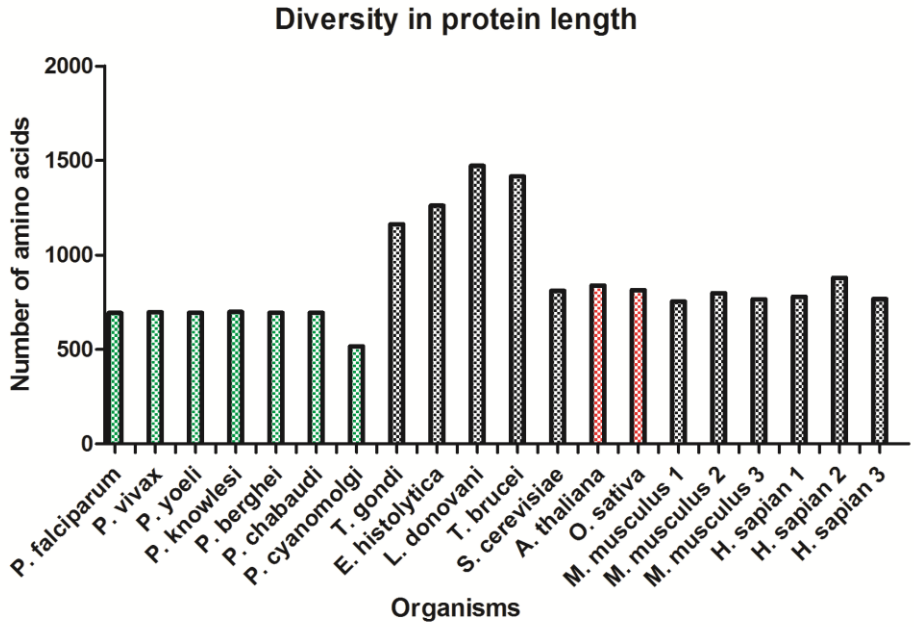

Figure 6.Diversity in protein length of AMPD from different organisms

AMPD of the genus *Plasmodium* has an average length of 695 amino acids, with AMPD from *P. cyanomolgi* being an exception, having only 516 residues. The protein from other protozoan parasites has been found to be comparatively long with as many as 1500 amino acids. AMPD from plants such as *Arabidopsis* and *Oryza* have a unique feature i.e. an N terminal trans-membrane helix that is not found in any other AMPD (*Han et al., 2006*). AMPD is encoded by a single gene in most of the unicellular eukaryotes, whereas multiple isoforms are found in mammals. Three isoforms present in mammals are skeletal muscle AMPD (AMPD1), soft tissue AMPD (AMPD2) and erythrocytic AMPD (AMPD3).

AMPD domain architecture comprises of a single domain characterised by an α_8/β_8 TIM barrel structure. This domain organization is the most common form of organization. But the AMPD proteins from few of the protozoan parasites such as *Acanthamoeba castellani, Entamoeba histolytica* etc. show whole domain duplication [Figure 7]. Nevertheless it is not known whether both the domains are catalytically active or not.

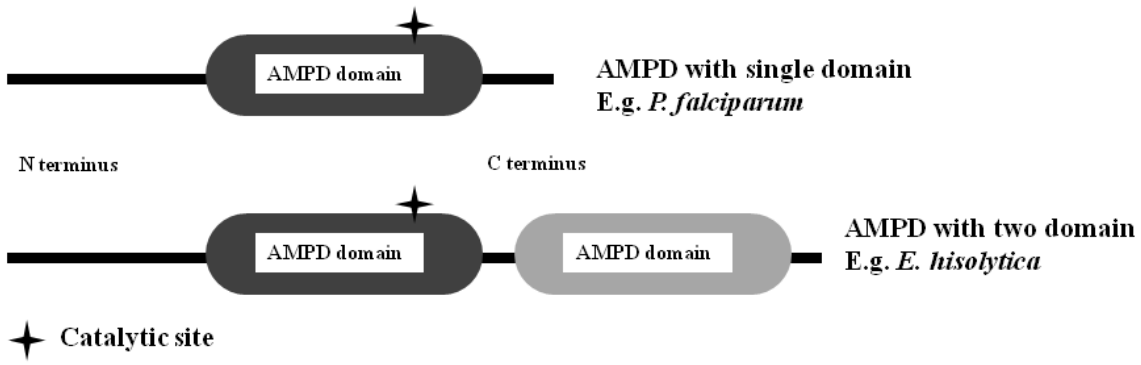

Figure 7.Schematic of domain organization of AMPD

The AMP deaminase enzyme regulates intracellular AMP levels by catabolising AMP to IMP. Impairment in this activity has physiological consequences. Accumulation of AMP leads to inhibition of *de novo* purine biosynthetic pathway enzyme glutamine PRPP amidotransferase, thereby shutting off purine biosynthesis through this pathway. This leads to depletion in levels of IMP which is a branch point metabolite that is needed for GMP production. Hence intracellular GMP levels and in turn GTP levels fall below optimum. Lack of GTP impairs protein production as GTP molecule is indispensible for translation initiation and elongation. As a consequence of this series of events, cells lacking AMPD activity show growth defect phenotype. This growth defect phenotype does not show up under normal conditions but reveals itself when cells are exposed to metabolite stress like presence of adenine (in case of yeast) or adenosine (in case of mammalian cells) in the media. AMP deaminase deficiency has been implicated in genetic disorder like myoadenylate deaminase deficiency where; mutations in skeletal muscle AMP deaminase gene lead to premature termination of translation and due to lack of functional enzyme, causes severe fatigue, muscle cramps in the subjects after performing trivial tasks like climbing stairs or walking across the hall. But evidences from literature also suggest lack of AMPD is not the only reason for this consequence. Mutations in AMPD2 have been identified in families where individuals were found to be suffering from a neurodegenerative brainstem disorder termed pontocerebellar hypoplasia. In these subjects neural cells in cerebellum and hippocampus die due to protein synthesis defect as a consequence of AMP accumulation caused by diminished levels of

AMPD2 enzyme (*Akizu et al., 2013; Chae et al., 2002; Haas et al., 2003 and Martini et al., 2007*).

The mechanism of catalysis for deamination reaction employs a conserved scheme of nucleophilic attack by a water molecule at the active centre co-ordinated by the divalent metal ion and hydrogen bonded by histidine and aspartate residues from the β strands [Figure 8]. Substrate binding initiates catalysis where activation of water molecule takes place by the general base histidine. The activated nucleophilic hydroxide ion attacks the carbon at the reaction centre resulting in the formation of tetrahedral reaction intermediate. This is followed by abstraction of a proton from a conserved general acid – glutamate. Now, the intermediate gets cleaved by general base catalysis performed by an aspartate residue, which deprotonates the carbinol intermediate. In the final step of catalysis proton is donated to the leaving NH_2 group, thereby forming ammonia, by the histidine residue and a new water molecule occupies the active centre (*Arbona, 2006*).

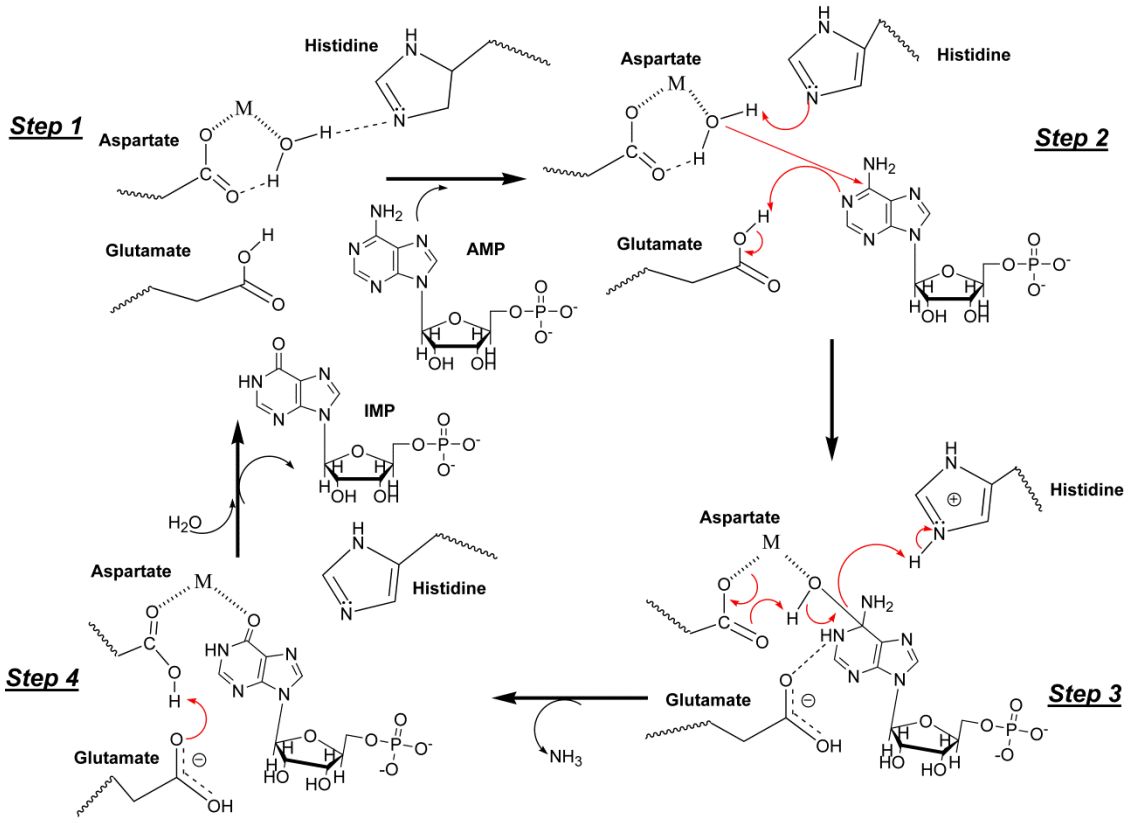

Figure 8.Reaction mechanism of AMP deamidation by AMPD

1.7 Preliminary bioinformatic analyses

AMPD is an exclusively eukaryotic enzyme and prokaryotes possess AMP nucleosidase which performs catabolism of AMP. In the Uniprot database there are 16 AMPD enzymes from different organisms including fungi, plants and mammals. But in the crystal structure database only one entry can be found, belonging to *Arabidopsis thaliana* (PDB ID 2A3L, this structure is of a truncated version of AMPD). The reason for this might be the protein's inherent tendency to undergo degradation at the N-terminal region and therefore its highly unstable nature. AMPD class of proteins are huge proteins with molecular weight >80kDa. The sequence diversity at the N-terminal region is a well known fact and has been reviewed by many authors (*Jurken and Sabina, 1995*). Also the existing reports on AMPD protein have been based on studies done on N-terminal truncated protein only (*Haas and Sabina, 2003; Meyer et al., 1989*). Properties like huge size, inherently disordered regions and propensity for degradation suitably entitle this protein as 'a crystallographer's nightmare'. Nevertheless this enzyme has important physiological consequences as described in the introduction. Hence studying this enzyme is a challenging and an interesting endeavour.

Plasmodium falciparum AMPDA (PfAMPD) has not been biochemically characterised. Sequence alignment was made with *Arabidopsis thaliana* AMPD (AtAMPD) and it was found that most of the residues involved in substrate binding and catalysis are highly conserved [Figure 9]. Structure was also generated by homology modelling technique using I-Tasser server, where AtAMPD was used as the template. The best homology was obtained with AtAMPD crystal structure based on good statistical parameters [Figure 10].

```
at              EMQDGVVHVFANKDAKEDLFPVADATAFFTDLHHVLKVIAAGNIRTLCHRRLVLLEQKFN 360
pf              ESNK-----LANHRN------IKSAEDYLSSIQEIMNVVQDPACKSFCFQRLKYLEKKFD 214
                * :.     :**:        : .*  :::.::.:::*:     :::*.:**  **:**:

at              LHLMLNADKEFLAQKSAPHRDFYNVRKVDTHVHHSACMNQKHLLRFIKSKLRKEPDEVVI 420
pf              FHIMFNGPLELSETRDIKHRDFYNIRKVDVHVHHSACMQQKELLRFIREKYRTEPNTVVY 274
                :*:*:*.  *:   :.  ******:****.********:**.*****:.* *.**: **

at              FRDG-TYLTLREVF-ESLDLTGYDLNVDLLDVHADKSTFHRFDKFNLKYNPCGQSRLREI 478
pf              INEKREMLTLKSIFDEELKSTAYESTIDTLGVNALGNCFHRFDLFNEKYNPFGQKLLRDI 334
                :.:    ***:.:* *.*. *.*: .:* *.*:*  . ***** ** **** **. **:*

at              FLKQDNLIQGRFLGEITKQVFSDLEASKYQMAEYRISIYGRKMSEWDQLASWIVNNDLYS 538
pf              FLKTDNYIEGRYLAEITKKQIKNLERSKYQHVEWRISIYGKNKNEWLKISKWVLNNQLSS 394
                *** ** *:**:*.****: :.:** **** .*:******:: .** :::.*::**:* *

at              ENVVWLIQLPRLYNIYKDMGIVTSFQNILDNIFIPLFEATVDPDSHPQLHVFLKQVVGFD 598
pf              IRVRWMIQVPRLYHIYKKMKLINTFADFLSNIFSPCFEAIKNPEENKEIFIFLHQIVGWD 454
                 .* *:**:****:***.* ::.:* ::*.*** * ***  :*:.: ::.:**:*:**:*

at              LVDDESKPERRPTK--HMPTPAQWTNAFNPAFSYYVYYCYANLYVLNKLRESKGMTTITL 656
pf              SVDDESIISNYTLKGGELPTPDKYVSEHNPPYSYYAYYMYINIRMLNEFMISRNMRPMAF 514
                 *****  .. . *  .:*** ::.. .**.:***.** * *: :**::  *:.* .:::

at              RPHSGEAGDIDHLAATFLTCHSIAHGINLRKSPVLQYLYYLAQIGLAMSPLSNNSLFLDY 716
pf              RPHCGEIGNMSHLACMFLLADRINHGINLRKSPVLLYLYYLKQIGLALSPLSNNALFLHI 574
                ***.** *::.***. ** .. * ********** ***** *****:******:***.

at              HRNPFPVFFLRGLNVSLSTDDPLQIHLTKEPLVEEYSIAASVWKLSACDLCEIARNSVYQ 776
pf              DKNPFKRFFKIGLNVTLSTDDPLMFHFTDEPLLEEYSICAHTWKLSTVDLCEIARASVIQ 634
                .:***  **  ****:******* :*:*.***:*****.* .****: ******* ** *
```

Figure 9.Partial sequence alignment of P. falciparum and A. thaliana AMPD with zinc binding residues highlighted in red and catalytic residues highlighted in green.

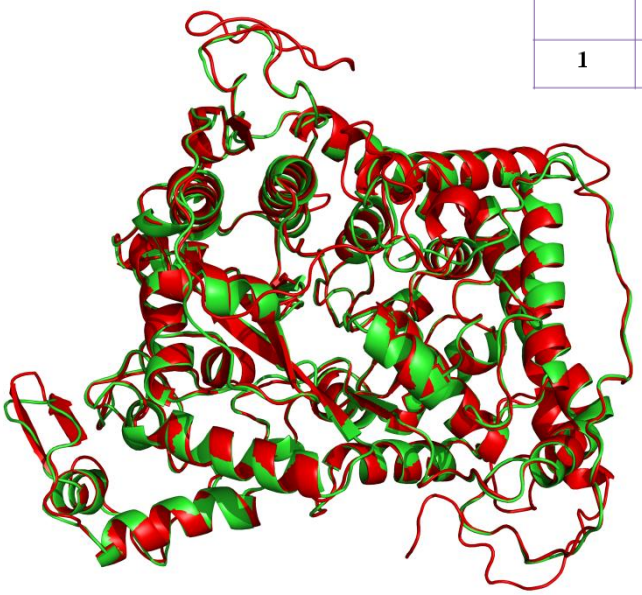

Rank	PDB Hit	Iden1	Tm Score	Cov.	Norm. Z-score
1	2A3L	0.43	0.87	0.88	3.68

Figure 10.Homology modelled structure of PfAMPD (red) superposed on AtAMPD (green). The statistical parameters are given in the box.

AMPD protein is known to show a very interesting mode of regulation. ATP is known to be the activator, whereas GTP, phosphate, phosphoinositides and polyamines are known to inhibit this enzyme. The anti-diabetic drug metformin is known to activate AMP activated protein kinase by direct inhibition of AMPD because AMPD inhibition leads to increase in AMP levels and AMP is a known activator of AMP activated protein kinase (*Merklers et al., 1989, 1990, 1993; Ouyang et al., 2011 and Xu et al., 2005*). AMPD is also known to be associated with myosin heavy chain (*Marquetant et al., 1989*) 'AMP deaminase' key word search in PubMed reveals 1925 publications but thorough biochemical characterization of a protozoan AMPD has not yet been done.

1.8 Objectives of the current study

AMPD protein from protozoan parasites has not been characterised. Since AMPD is a chief enzyme of purine nucleotide cycle and also a vital regulator of adenylate kinase activity, thereby regulating AEC of a cell; it would be very interesting to determine the role of AMPD enzyme in the apicomplexan parasite *P. falciparum*. In this regard following objectives were set for our study:

- Cloning, expression and purification of recombinant PfAMPD
- Biochemical and biophysical characterization of PfAMPD by spectral investigations
- Elucidation of physiological role of PfAMPD

Chapter 1	• Introduction
Chapter 2	• **Expression of PfAMPD in *E. coli* and yeast**
Chapter 3	• Localization studies in *P. falciparum*
Chapter 4	• Complementation studies in AMPD knockout yeast strain

Chapter 2 – Expression of PfAMPD in *E.coli* and yeast

Requirement of a purified protein is indispensible for its biochemical and biophysical studies. Hence attempts were made to express and purify recombinant PfAMPD from heterologous expression systems like *E. coli* and yeast, *S. cerevisiae.*

2.1 Materials and methods

All chemicals and reagents were procured from Sigma Aldrich, USA; Fischer chemicals, USA and media components were purchased from Himedia, Mumbai. Primers for cloning were obtained from Sigma Aldrich, India (all primer sequences have been provided in the appendix). Restriction enzymes, Phusion polymerase, T4 DNA ligase were obtained from New England Biolabs, USA and Moloney Murine Leukemia Virus reverse transcriptase was purchased from GE Life Sciences, India and used according to manufacturer's instruction. Antibodies were procured from Sigma Aldrich, USA and Bangalore Genie, India. Cloning strains XL-1 blue, XL-10 gold and bacterial expression strains BL21 (DE3) Rosetta (DE3) pLysS, BL21 (DE3) RIL and plasmids pETDuet-1 and pET28d were from Novagen, India. Ni-NTA agarose matrix was purchased from Thermo Scientific, India. Plasmid isolation and PCR purification kits were from Qiagen, Netherlands. Trizol reagent for RNA isolation was procured from Invitrogen, USA. Wild type yeast strain BY4742 (*MATα; his3Δ 1; leu2Δ 0; lys2Δ 0; ura3Δ 0*) and pYES2/CT plasmid were kind gifts from Dr. Ravi Manjithaya, MBGU, JNCASR and Prof. G. Padmanabhan, Department of Biochemistry, Indian Institute of Science, Bangalore. Gene sequencing by the Sanger sequencing method was carried out in the in house sequencing facility, JNCASR, Bangalore.

2.1.1 RNA isolation

Saponin released intraerythrocytic *P. falciparum* from 40mL of in vitro culture were treated with 1mL Trizol reagent at room temperature for 15 minutes and then centrifuged for 30

minutes at 18000×g to remove the cell debris. The supernatant was transferred to a fresh tube and 200µL of chloroform was added and kept at room temperature for 15 minutes. This was centrifuged at 18000×g for 30 minutes at 4℃ for phase separation. The top layer was aspirated to a fresh tube and 400µL of isopropanol was added and kept at -20℃ for 4 hrs. This was centrifuged at 18000×g for 30 minutes at 4℃ to obtain an RNA pellet. This was washed once with 75% ethanol made in diethylpyrocarbonate (DEPC) treated water and allowed to air dry. The pellet was resuspended in 20 µL of DEPC treated water and stored at -80℃.

2.1.2 cDNA synthesis, cloning and transformation

Since PfAMPD had seven introns, in order to facilitate cloning the cDNA was synthesised using the primer ***pfampd-rp_hindiii*** (see appendix for sequence) and Moloney Murine Leukemia Virus reverse transcriptase. This cDNA was used as template for PCR amplification of PfAMPD gene using the primers ***pfampd-fp_ecori*** and ***pfampd-rp_hindiii*** (see appendix for sequence). The PCR product was digested with EcoRI and HinDIII enzymes and ligated to the first multiple cloning site of pETDuet1 (see appendix for plasmid map) vector to give an N-terminal $(His)_6$ -tagged construct and transformed into competent XL-1 Blue *E. coli* cells. The transformants were selected on LB plate containing 100µg/mL ampicillin. The transformants were screened by standard protocols (mobility shift of the super coiled plasmid, insert release, PCR and sequencing). Three N – terminal truncated versions of PfAMPD- Δ59, Δ94 and Δ178 were constructed using forward primers ***Δ59 ampda ecori fp, Δ94 ampda ecori fp*** and ***Δ178 ampda ecori fp*** respectively and a common reverse primer ***pfampd-rp_hindiii*** (see appendix for sequence)**.** The full length construct served as template and all three truncated constructs were made in pETDuet1 vector and transformed into competent XL-1 Blue *E. coli* cells. A C-terminal $(His)_6$ -tagged construct was generated in plasmid pET28d (see appendix for vector map) using primers ***ampd c term-***

fp - nco1 and ampd c term-rp – xho1 (see appendix for sequence)**.** Since PfAMPD gene consisted of NcoI site, site directed mutagenesis was performed to remove this site to facilitate cloning.

2.1.3 Site directed mutagenesis

Overlap PCR method was adopted to introduce silent mutations which would facilitate cloning of PfAMPD into pET28d vector. PfAMPD was PCR amplified using full length clone as template and primer pairs ***ampd c term-fp - nco1, ampd ol-ir*** and ***ampd ol-if, ampd c term-rp - xho1***(see appendix for sequence) to generate two amplicons which have a 32 base pair overlap region where the mutation has been introduced. These two amplicons were now used as template and amplified using ***ampd c term-fp - nco1*** and ***ampd c term-rp - xho1*** primers to generate the full length AMPD gene. This PCR product was digested with NcoI and XhoI enzymes and ligated to pET28d plasmid and transformed to competent XL-1 blue cells. Clones were confirmed by standard protocols.

2.1.4 Protein expression in E. coli

Plasmid was isolated from the positive clones and transformed to Rosetta (DE3) pLysS and BL21 (DE3) RIL strains and expression was checked under various conditions. A single colony was inoculated in to 10mL terrific broth and grown overnight at 37 ℃ in a shaker incubator. To fresh TB media, 1% overnight culture was added as inoculum and grown till 0.6 OD at 37℃. The culture was induced using 0.5mM IPTG and incubated for further 6hrs. For solubility check the cells were lysed by sonication (5 seconds pulse, 5 seconds pause, 5 minutes) and the lysates was spun at 18000×g for 20 minutes at 4 ℃. Pellet and supernatant fractions were analysed by SDS-PAGE and Western blot using anti-$(His)_6$ antibodies.

2.1.5 *Bacterial cell lysis and protein purification under denaturing conditions*

The induced culture (1 ltr) was harvested by centrifugation for 10 minutes. The culture pellet was resuspended in 20mL lysis buffer 20 mM Tris HCl, pH7.4, 100 mM NaCl, 10 % glycerol, 0.1 mM PMSF and lysed by passing through French pressure cell four times. The lysate was centrifuged at 16000×g, 4℃ for 30 minutes. The lysate pellet was resuspended in denaturing buffer 20 mM Tris HCl, pH7.4, 100 mM NaCl, 10 % glycerol, 0.1 mM PMSF, 6 M guanidinium chloride (GdmCl) and kept for tumbling overnight. The lysate was centrifuged at 18000×g, at room temperature for 30 minutes. The supernatant was mixed with 1mL of Ni-NTA beads and kept for tumbling for 3hrs at room temperature. The lysate along with beads was poured on to a column. The flow through was collected followed by washing with wash buffer 20 mM Tris HCl, pH7.4, 100 mM NaCl, 10 % glycerol, 0.1 mM PMSF 6M GdmCl, 20mM imidazole. The bound protein was eluted using elution buffer 20 mM Tris HCl, pH7.4, 100 mM NaCl, 10 % glycerol, 0.1 mM PMSF 6M GdmCl containing 250 or 500 mM imidazole. Final elution was done with 0.2 M EDTA containing buffer. The fractions were analysed on 10% SDS-PAGE and Western blot was done to detect the protein by probing with anti-$(His)_6$ antibody.

2.2 Methods in yeast

2.2.1 Cloning and transformation

Shuttle vectors were used for their ease of cloning in *E. coli* and ability to express genes of interest in yeast. PfAMPD was cloned in to yeast expression vector pYES2/CT (see appendix for vector map), a 2μ plasmid with a *Gal1* promoter, using ***pyes ampd fp kpn1*** and ***pyes ampd rp xba1*** primers (see appendix for sequence). Clone was confirmed by standard protocols and transformed to wild type yeast BY4742 strain by LiAc/SS carrier DNA/PEG method (*Dainel Gietz et.al, 2007*). Single colony was inoculated in YPD medium for primary

culture and incubated at 30 °C, 250 rpm and allowed to grow overnight. The OD was checked at 600 nm and 1 OD cells were transferred to 5 ml YPD medium and allowed to undergo 2 doublings (4 hrs - 5 hrs) at 30 °C, 250 rpm to get a final OD of 4. Transformation mix was prepared by aliquoting the following reagents into a sterile eppendorf tube - 50%PEG-3350 240 µL, 2mg/ml Carrier DNA 50 µL (boiled and snap cooled before adding), 1M Li acetate - 36 µL, PCR product/PLASMID (1µg) 10-15 µL and Water 24-19 µL. Cells were harvested by centrifugation, washed twice with water and 360 µL of transformation mix was added and mixed thoroughly avoiding any clump formation. Heat shock was given at 42℃ for 40 minutes. After heat shock the cells were harvested by centrifugation, resuspended in 100 µL water and plated on SD minus (-) uracil (SD-synthetically defined) plates and grown at 30℃ for three days. Secondary plating was done and colonies were screened by isolating genomic DNA by single tube lithium acetate-SDS method (*Looke et al., 2011*) and performing PCR.

2.2.2 Yeast genomic DNA isolation

Single colonies of *Saccharomyces cerevisiae* were picked from a plate, resuspended in 100 µl of 200 mM lithium acetate, 1% SDS solution and incubated at 70°C for 15 minutes. After incubation, 300 µl of 96% ethanol was added for DNA precipitation, samples were mixed by brief vortexing and DNA was collected by centrifugation at 15000g for 3 minutes. Precipitated DNA was dissolved in 100 µl of sterile water, cell debris was spun down by brief centrifugation (15000g; 1 minute) and 1 µl of the supernatant was used for PCR (*Looke et al., 2011*).

2.2.3 Expression and protein purification from yeast

Positive colony was inoculated to SD-uracil liquid media containing glucose as carbon source, grown overnight, harvested the next day and washed with sterile water followed by transfer to SD-uracil media containing galactose as carbon source. Galactose acts as an

inducer and induction was carried for 20 hrs at 30℃. Cells were harvested by centrifugation and resuspended in lysis buffer containing 20mM Tris HCl, pH 7.4, 100 mM NaCl, 10% glycerol and 0.1 mM PMSF. By freeze thawing using liquid nitrogen and mechanical grinding using mortar and pestle, the cells were lysed. The lysates were centrifuged at 18000×g for 30 minutes; the supernatant was separated and mixed with nickel-NTA sepharose beads. This mixture was incubated at 4℃ for 3 hrs and thereafter washed using wash buffer 20mM Tris HCl pH7.4, 100 mM NaCl, 10% glycerol, 20 mM imidazole and 0.1 mM PMSF. Protein was eluted using buffer 20 mM Tris HCl, pH 7.4, 100 mM NaCl, 10% glycerol 0.1 mM PMSF containing 250, 500 mM imidazole and 0.2 M EDTA separately. Fractions were loaded on SDS-PAGE gel and Western transfer was performed and the blot was probed with anti-$(His)_6$ primary antibody from mice, followed by goat anti-mice secondary antibody conjugated to horse radish peroxidise (HRP). Development was done by the chemiluminescence method.

2.3 Results and discussion

RNA isolation, cDNA synthesis and PCR amplification of PfAMPD

RNA was isolated from the saponin released parasites to avoid contamination by globin mRNA of erythrocytes. This was used as template for the reverse transcriptase reaction to generate cDNA. Using this cDNA as template and gene specific primers full length PfAMPD gene was PCR amplified. Since the yield was poor, the amplicon was eluted from the gel and used as template for 3-4 rounds of PCR to generate enough amplified product for restriction digestion and cloning (data not shown).

Generation of $(His)_6$ -tagged constructs of PfAMPD

Full length and truncated versions of PfAMPD were cloned into pETDuet-1 vector to generate N-terminal $(His)_6$-tagged constructs. Confirmation of clones was done by standard

protocols as mentioned earlier. Restriction digestion of the plasmid containing PfAMPD was done and the samples were subjected to electrophoresis on 0.8% agarose gel. Visualization was done by ethidium bromide staining [Figure 11]. In order to fuse $(His)_6$ at the C-terminus of PfAMPD, the gene was cloned into pET23d vector between NcoI and XhoI sites. Since PfAMPD had an internal NcoI site, an overlap PCR strategy [Figure 12A, B and C] was adopted to remove the site and then cloning was performed. Clone was confirmed by insert release and was partly sequenced [Figure 12D].

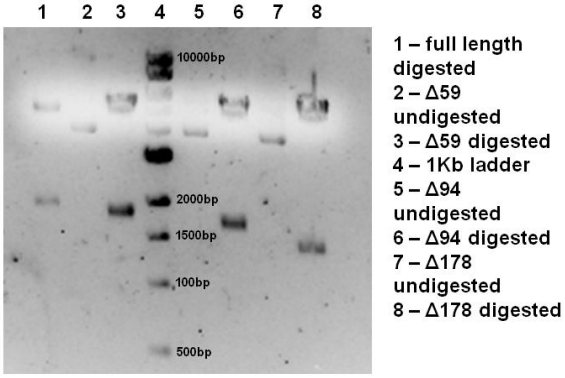

Figure 11.Confirmation of N-terminal $(His)_6$-tagged constructs of PfAMPD by restriction digestion with EcoRI and HinDIII. DNA samples loaded in different lanes are indicated in the image. Various deletion constructs are described in the text.

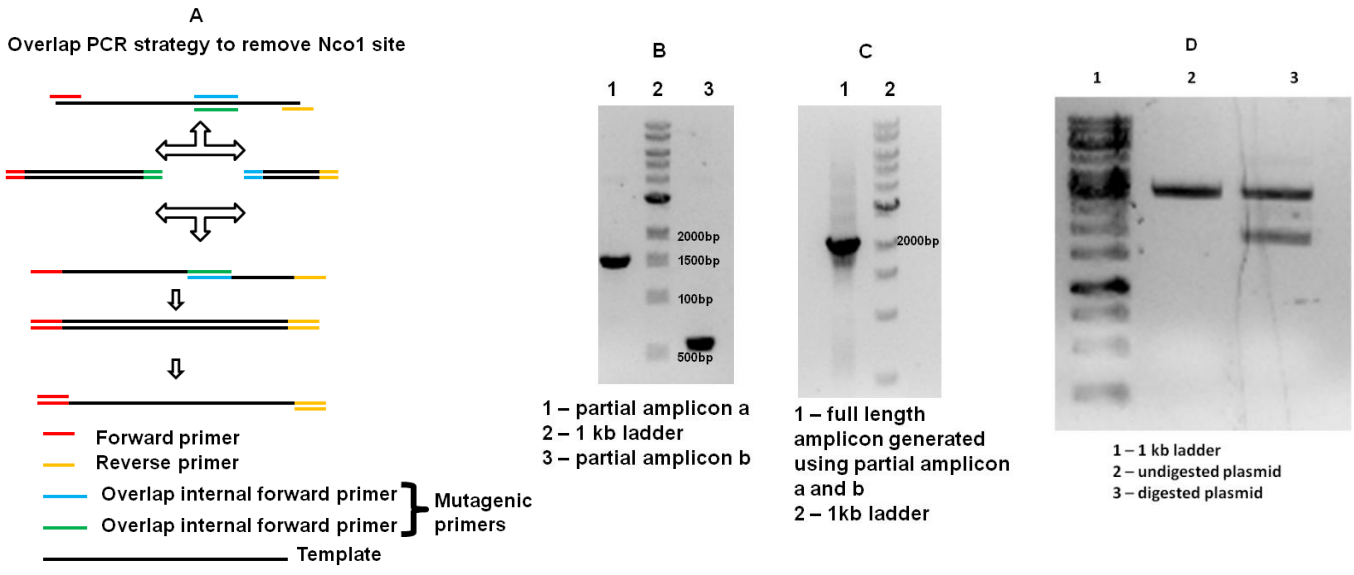

Figure 12.Cloning of C-terminal $(His)_6$-tagged PfAMPD in pET23d. (A) Schematic representation of the strategy used to delete the single NcoI site in PfAMPD gene. Agarose gel electropherogram of (B) N-term and C-term fragments of PfAMPD generated by PCR, (C) full length gene of PfAMPD generated by PCR with internal NcoI site deleted and (D) NcoI, XhoI digested plasmid DNA isolated form one of the positive clones. Samples loaded in the lanes are indicated in the figure.

Expression of PfAMPD with N-terminal $(His)_6$ -tag in E. coli

Expression of PfAMPD was carried out in BL21 (DE3) RIL and Rosetta (DE3) pLysS strains. These strains are T7 promoter based expression systems and are also codon optimised. PfAMPD gene is an AT rich gene (70%AT) and contained high number of rare codon (72), hence codon optimised expression strains were used for optimum protein expression. Expression was carried out as mentioned in the methods and samples were analysed by SDS-PAGE electrophoresis and visualization was done by Coomassie staining and Western blot (Figure 13A and B).

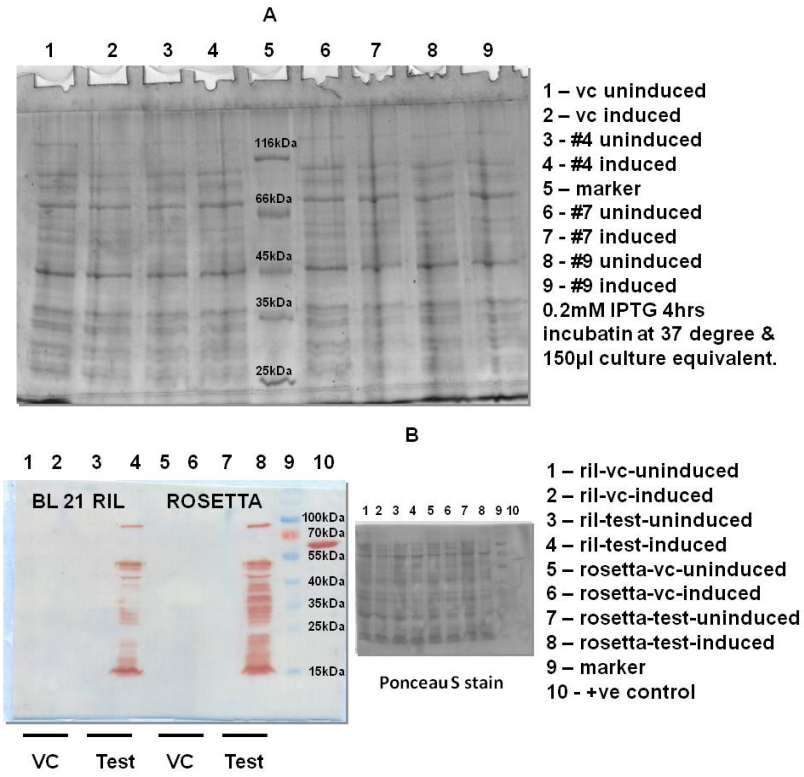

Figure 13.Expression check of PfAMPD. (A) SDS-PAGE profile of whole cell lysates of VC (vector control) and different clones of N-term $(His)_6$ -tagged full length PfAMPD and (B) Western blot of whole cell lysates after short induction protocol. PonceauS stained blot has been shown as loading control. Samples loaded in different lanes are indicated in the image.

Upon Coomassie staining no difference was observed between vector control and test under uninduced and induced conditions. Several other conditions like lower temperature and different IPTG concentrations were tried; nevertheless the profile on the gel remained the same. With protein degradation being the prime suspect, a short induction protocol was

followed and Western blot was performed by semi dry technique using whole cell lysates and probed with commercial anti-HIS primary antibody from mice and goat anti-mice HRP conjugated secondary antibody.

Western blot revealed the presence of a full length band around 83kDa and a battery of peptides of lower molecular weight, indicating the protein might be getting degraded by proteolysis. Solubility check was performed by lysing the cells using sonicator and it was found that the full length and the lower molecular weight bands went in to inclusion bodies and were absent in the lysate supernatant [Figure 14A]. It was also found that the protein was not soluble in buffer containing the denaturant, urea (3M and 6M). The protein was found to be soluble only in buffer containing 6M GdmCl [Figure 14B].

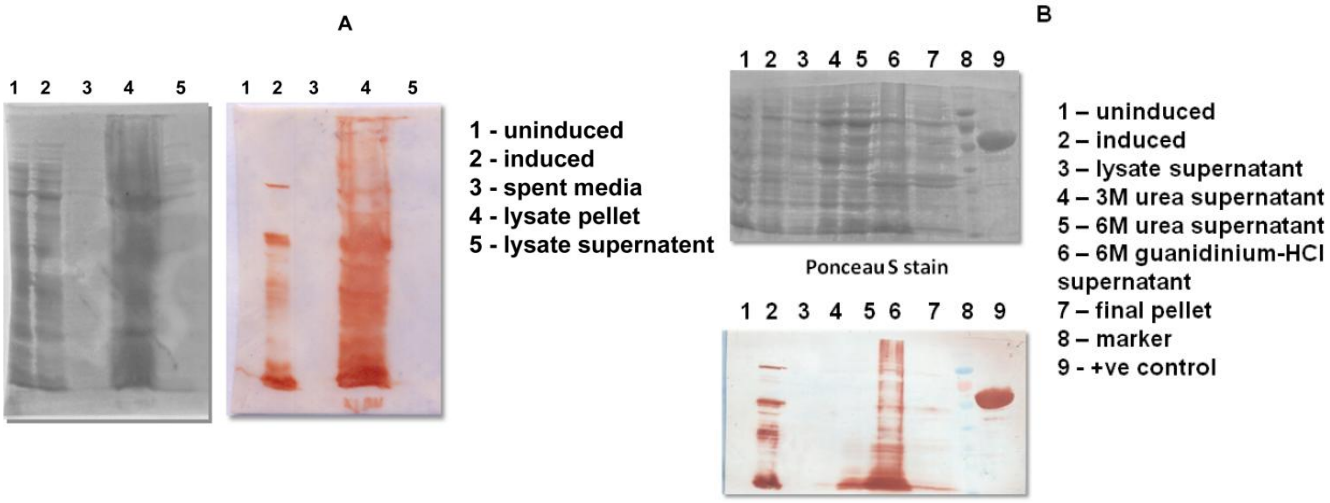

Figure 14.Solubility check of PfAMPD. (A) Western blot profile showing presence of PfAMPD in insoluble fraction. Urea and GdmCl were used to denature and solubilise the protein. (B) Western blot showing solubility of the protein in 6M GdmCl. Samples loaded in different lanes are mentioned in the image. Marker is as described in figure 12B.

Immobilised metal ion affinity chromatography was performed to purify the protein under denaturing conditions using Nickel – NTA beads (Thermo Scientific). And elution was performed with different concentration of imidazole and EDTA containing buffer. The eluates were analysed by SDS-PAGE electrophoresis and Western blot [Figure 15]. The purification profile is as shown in Figure 15 and it was found that full length and lower

molecular weight fragments get purified by virtue of the $(His)_6$ tag. Hence the purified fractions are not homogenous.

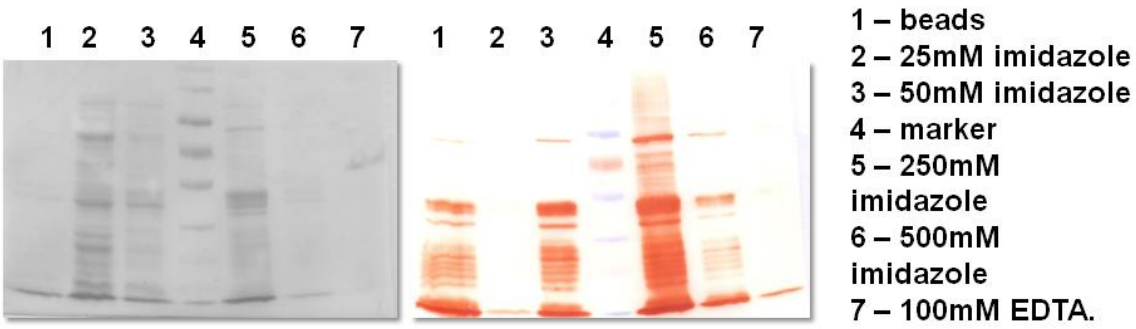

Figure 15.Western blot of eluates of N-term $(His)_6$ –tagged PfAMPD after nickel NTA chromatography. Samples loaded in different lanes are indicated in the image. PonceauS stained blot is shown in left panel. Marker is as described in figure 12B.

Using the purified protein refolding experiments were attempted by diluting the denaturant and by matrix assistance. But both techniques failed as the protein precipitated upon removal of denaturant. The N-term $(His)_6$ -tagged construct did not yield stable and soluble protein and hence it was decided to make N-terminal truncated versions of the PfAMPD in order to get a stable soluble protein.

Expression of N-term deleted PfAMPD

AMPD class of proteins is known to have a diverse N-terminal sequence and it is also known to be highly unstable and prone to proteolytic degradation. So far in the literature the biochemical characterisation has been done only on N-terminal deleted AMPD. Hence it was decided to generate truncated versions of PfAMPD. The basis of the truncation was the sequence alignment with AtAMPD protein [Figure 16], whose structure has been deposited in PDB database (PDB ID 2A3L).

Full length AtAMPD was found to be insoluble as it was predicted to possess an N-terminal transmembrane helix. But a crystal had been obtained from a truncated version (Δ139). Even in this crystal, electron density was not obtained for the initial 60 residues indicating that this

region might be disordered. So, our first truncation was based on the alignment between Δ139 of *Arabidopsis* and *P. falciparum* AMPD. This was Δ59 in case of PfAMPD.

Further analysis of the crystal structure showed that an N-terminal stretch of 73 residues was missing in the electron density map. Therefore electron density in the structure begins from residue 212. However initial 35 residues exhibited a random coil structure. Therefore our second deletion construct lacked the first 94 residues in the aligned PfAMPD. Our second truncated version Δ94 corresponds to the region on Arabidopsis protein from which the first α-helix starts.

One more truncation Δ178 was made which comprised of the protein which aligned with the catalytic core of the *Arabidopsis* AMPD starting from α helix-3. All constructs were made in pETDuet1 vector and transformed to Rosetta (DE3) pLysS strain and expression was checked by Western blotting.

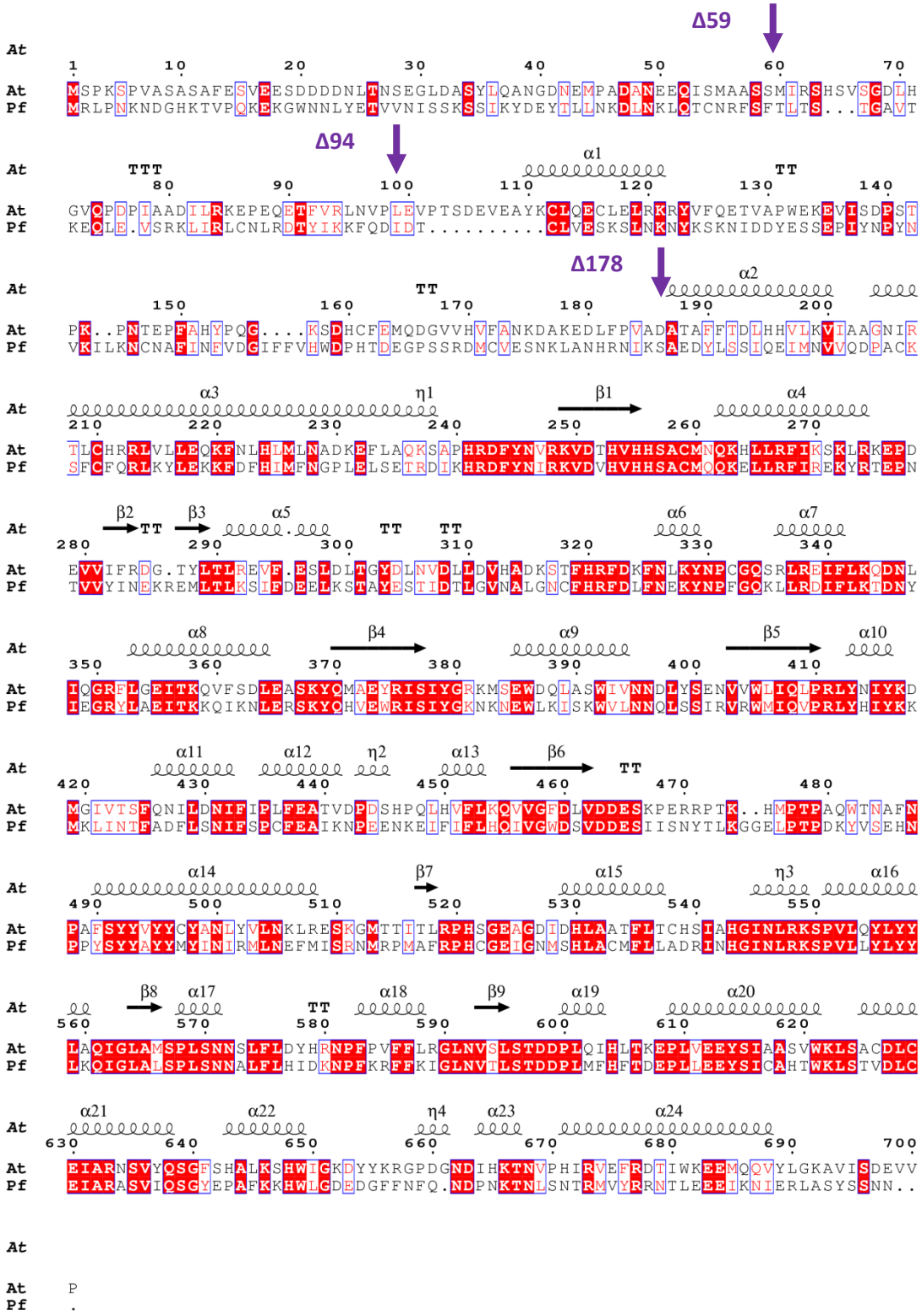

Figure 16.ClustalW alignment of AtAMPD and PfAMPD showing conserved residues in red and secondary structures. Specific points of deletion are indicated by arrows.

Three truncated forms of PfAMPD were made and expression and solubility were determined for all three [Figure 17]. All three constructs were found to show a similar pattern when compared to full length protein. A full length band and a battery of lower molecular weight bands were seen. Also solubility check was performed after lysis of the cells and it was found that all three truncated versions went in to inclusion body i.e. insoluble fraction.

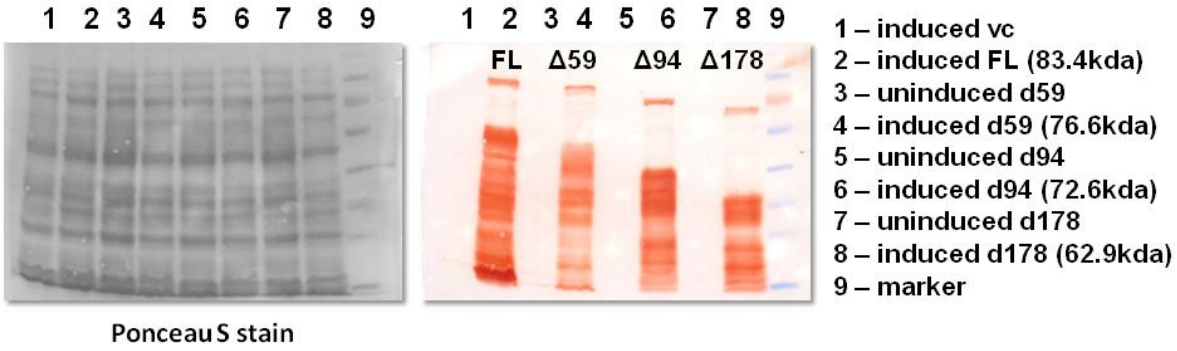

Figure 17.Western blot profile of the full length PfAMPD and three truncated constructs. Marker is as described in figure12B.

The 'protein degradation or ribosome stalling' conundrum

The appearance of both full length and lower molecular bands which were Western blot positive provoked the question that whether the observation was a result of protein degradation by proteolysis inside the cells or was it due to ribosome stalling which occurs as a result of presence of abundant rare codons in the gene of interest. In order to address this, two experiments were designed. One involved induction of protein followed by analysis of aliquots taken at different time points by Western blot. If the protein was indeed getting degraded then there should be a negative correlation between the band intensity and duration of induction. The second experiment was akin to a pulse chase experiment, where protein was induced for a short duration followed by global arrest of translation using an antibiotic (tetracycline in our case). Then aliquots were taken at different time points after arrest of translation and analysed by western blot. If ribosome stalling was the culprit responsible for

the lower molecular weight bands then similar band intensity should be maintained till the last time point.

The above described experiments were performed and samples were analysed by Western blot. The profile from the first experiment showed that during the later time points there were no Western blot positive protein bands indicating that the cause of the lower molecular weight bands might be proteolytic degradation [Figure 18 left panel]. Whereas the second experiment showed that after arrest of translation the levels of Western blot positive protein bands were maintained at more or less same levels suggesting the possibility of ribosome stalling being the cause for appearance of lower molecular weight bands [Figure 18 right panel]. Nevertheless this set of experiments was inconclusive as it indicated the possibility of both ribosome stalling and protein degradation as the potential cause of the lower molecular weight bands which we see upon induction of PfAMPD.

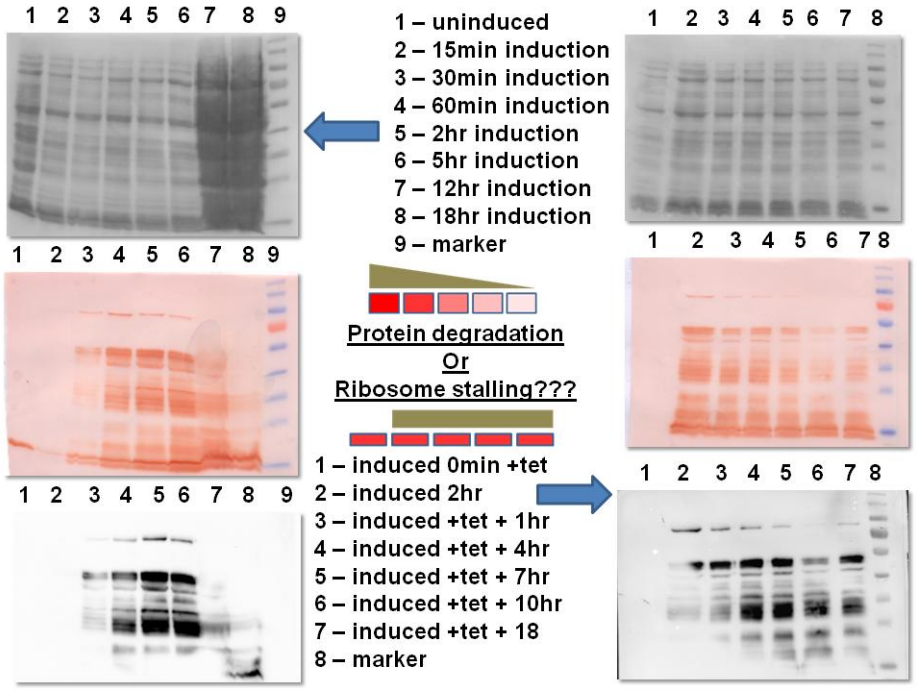

Figure 18.Experiment to validate protein degradation (top panel) or ribosome stalling (bottom panel) as cause of occurrence of multiple lower bands upon induction of PfAMPD. Top image is PonceauS stained blot, central image is colorimetric method of development and bottom image is blot developed by chemi-luminescence method of development. Schematic representations of both phenomena are given at the centre of the image.

Expression of C-terminal $(His)_6$ tagged PfAMPD

Since the previous experiments were neither conclusive in answering what caused the appearance of lower molecular weight bands, nor in obtaining a soluble homogenous stable protein, a C-terminal $(His)_6$ -tagged construct was made in the plasmid pET23d, transformed to Rosetta (DE3) pLysS strain and expression was checked by SDS-PAGE and Western blot. The reason for making this construct was that even if ribosome stalling happened, then the stalled products will not bear the tag. But the full length band unlike the fragments will have the tag, be western blot positive and therefore can be purified to homogeneity.

Upon Western blot analysis it was found that even the C-term $(His)_6$ -tagged construct showed full length and lower molecular weight bands. This concluded that indeed protein was getting degraded. The purification was done under the denaturing conditions like the N-term $(His)_6$ -tagged construct and this also gave a heterogeneous population of full length and degraded PfAMPD [Figure 19]. Both the Ponceau and the western blot show that the C-term $(His)_6$ -tagged protein purified under denaturing conditions is significantly purer than the N-terminal $(His)_6$ -tagged protein.

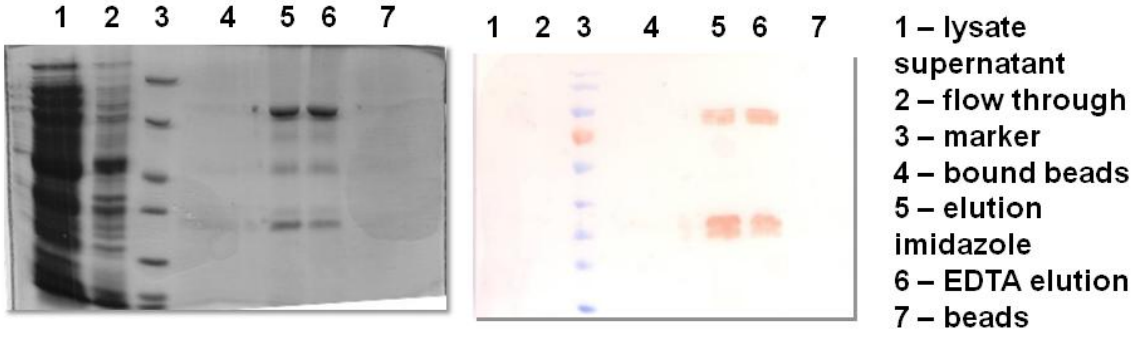

Figure 19.Purification profile of C-term $(His)_6$ -tagged PfAMPD under denaturing conditions. Marker is as described earlier. Coomassie stained gel has been shown on left as loading control.

Expression of C-terminal $(His)_6$ -tagged PfAMPD in yeast

Upon expression and purification using yeast expression system the protein was found to be present in soluble fraction. Full length and few N-term truncated bands were observed

indicating the unstable nature of PfAMPD. However due to the poor yield activity measurements could not be conducted [Figure 20].

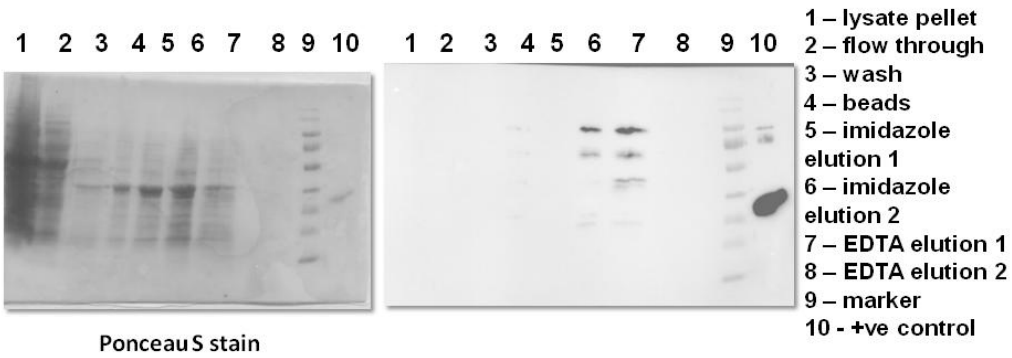

Figure 20.Purification profile of PfAMPD using yeast as expression system

Several attempts were made to increase cell density which would help in increasing protein yield but this objective was not accomplished and the above shown result was not reproduced.

Chapter 1	• Introduction
Chapter 2	• Expression of PfAMPD in *E. coli* and yeast
Chapter 3	• **Localization studies in *P. falciparum***
Chapter 4	• Complementation studies in AMPD knockout yeast strain

Chapter 3 – Localization studies in *P. falciparum*

In vivo localization forms a vital part of study of a particular protein as it can give information regarding its function as well as sequence specific features, such as membrane association. Performing localization studies for a given protein requires either specific antibodies or the gene to be tagged with a fluorophore like GFP; RFP etc; both these strategies were adopted for PfAMPD.

3.1 Materials and methods

All chemicals and reagents and media were procured from Sigma Aldrich, USA; Fischer chemicals, USA. Primers for cloning were obtained from Sigma Aldrich, India. Restriction enzymes, Phusion polymerase, T4 DNA ligase were obtained from New England Biolabs and used according to manufacturer's instruction. Alexa 488 tagged antibodies were procured from ABcam, England. Cloning strains XL-10 gold and bacterial expression strains Rosetta (DE3) pLysS, pET28d plasmid were from Novagen, India. Ni-NTA agarose and protein G sepharose matrix was purchased from Thermo Scientific, India and GE life sciences, India respectively. Plasmid isolation and PCR purification kits were from Qiagen, Netherlands. Plasmid pGLUX was a kind gift from Prof. Alan F. Cowman, Melbourne. Confocal microscopy was carried out in the in house central instrumentation facility, JNCASR, Bangalore. Blood required for parasite culture was collected from healthy individuals having O+ve blood group. Ethical clearance for this purpose has been obtained from the institutional committee. New Zealand white female rabbit was provided by the animal facility to generate antigen specific antibody.

3.1.1 Antigen purification and immunization

For this purpose PfAMPD C-term $(His)_6$- tagged construct was used. The protein was expressed in Rosetta (DE3) pLysS strain and purified under denatured conditions. The

protein was ethanol precipitated and run on SDS-PAGE, followed by coomassie staining. The full length band and the major degradation band at around 35kDa was cut and minced into small bits and electroelution was performed using SDS-PAGE buffer 25 mM Tris HCl, 192 mM glycine, 0.1% SDS, followed by electrodialysis using 15 mM ammonium bicarbonate buffer containing 0.0125% SDS. This sample was lyophilized and then resuspended in 1xPBS and quantified calorimetrically by Bradford's method. This was used as antigen to immunise New Zealand White rabbit in order to generate antibodies. The immunization schedule was as follows - pre immune collection – day 0; Primary injection – day 1 (400µg antigen with Freund's complete adjuvant); 1st booster – day 15 (250µg antigen with Freund's incomplete adjuvant); 2nd booster – day 30 (200 µg antigen with Freund's incomplete adjuvant); Test bleed – day 37; 1st major bleed – day 40; 3rd booster – day 70 (200 µg antigen with Freund's incomplete adjuvant); Test bleed – day 7 and Major bleed – day 78. Blood collected from the rabbit was allowed to clot overnight at 4℃. Later it was centrifuged and the supernatant antisera was collected and stored in aliquots at -20℃.

3.1.2 Dot blot

1-2 µg of antigen was spotted on the nitrocellulose membrane and allowed to dry for 15 minutes. Nitrocellulose membrane was blocked with 5% skimmed milk in 1xPBS for 1h on a rocker at room temperature. 5% skimmed milk was removed and 2.5% skimmed milk in 1xPBS containing different dilution of primary antibody was added. This was incubated on rocker for 1h at room temperature. The blots were washed for 15 minutes in 1xPBS containing 0.1% Tween 20. 2.5% skimmed milk containing 1:4000 dilution of secondary antibody was added and kept on rocker for 1h at room temperature. Blots were again washed for 15 minutes in washing solution. Blots were developed using coloring reagent aminoethylcarbazole.

3.1.3 Antibody purification

Since PfAMPD protein was insoluble conventional antibody purification protocol could not be followed. Hence strip affinity protocol was followed to purify antigen specific antibody, which was subsequently used for indirect immunofluorescence using confocal microscopy. Denatured and purified PfAMPD was precipitated by treatment using 90% ethanol overnight. The precipitate was centrifuged, dried and resuspended in 1X SDS-PAGE loading dye and boiled for 5 minutes. The sample was subjected to SDS-PAGE and Western transfer. The blot was PonceauS stained and the bands of interest were cut and blocked by using 5% skimmed milk in 1xPBS. The blots were then incubated with antiserum overnight at 4℃ and washed three times with 1xPBS containing 0.1% Tween20. Antibody bound to the blot was eluted using 100 mM Tris-glycine, pH 2.5 and immediately neutralised using 1 M Tris HCl, pH 8.0. This was repeated and the fractions eluted were concentrated using centrifugal concentrators.

Antibodies were also purified by using protein G sepharose beads. The antiserum was incubated with 100µL of protein G sepharose slurry overnight at 4° C. After incubation the beads were separated and washed with 1X PBS containing 0.1% Tween 20. Antibody bound to the beads was eluted using 100 mM Tris-glycine, pH 2.5 and immediately neutralised using 1 M Tris HCl, pH 8.0. This was repeated and the fractions eluted were concentrated using centrifugal concentrators.

3.1.4 Parasite culture methods

Fresh blood (O+ve blood group) was collected from volunteers and stored in the presence of the anticoagulant, acid citrate dextrose solution at 4℃ overnight. Plasma was separated and discarded. The erythrocytes were washed with 1x PBS three times and stored at 4 ℃ in incomplete RPMI media containing 25mM HEPES at 50% hematocrit in the presence of antibiotic gentamycin 2.5 µg/mL. Parasites were grown using complete RPMI media (20

mM glucose, 0.2% sodium bicarbonate, 0.5% Albumax and 50 μM hypoxanthine) at 5% hematocrit under micro-aerophillic conditions using candle jar setup at 37℃. Parasitemia was checked regularly by making Giemsa stained smears. 5-10% parasitemia was maintained and media change was given daily.

3.1.5 Saponin release of parasites

40 mL parasite culture was centrifuged in a falcon for 10 minutes at 2000×g and supernatant was removed. To 1 volume of erythrocyte pellet 2 volumes of saponin solution was added (0.15% saponin in 1x PBS). Components were mixed gently (without making any bubble), incubated at room temperature for 5 minutes and centrifuged at 2000×g for 40 minutes. Supernatant was removed. Free parasites were washed twice with 1x PBS and were flash-frozen in liquid nitrogen and stored at -80℃.

3.1.6 Indirect immunofluorescence

0.5 ml of parasite culture was pelleted and washed with 1x PBS. This was fixed with 4% paraformaldehyde and 0.0075% glutaraldehyde for 30 minutes at room temperature followed by washing with 1x PBS. Fixed parasites were permeabilized with 0.08% TritonX-100/1xPBS for 9 minutes and washed with 1x PBS. Permeabilized cells were blocked in 3% BSA/1xPBS for 1h at room temperature on a tumbler. Primary antibody (1:500)/3% BSA/1xPBS was added to the cells and kept for tumbling for 1h at room temperature followed by 1x PBS wash. Secondary antibody (1:1000)/ 3% BSA/1xPBS was added to the cells and kept for tumbling for 1h at room temperature. Also propidium iodide (1μg/ml) was added at this step itself. The cells were then washed with 1x PBS and resuspended in 70% glycerol. Cells were mounted on glass slide using the poly L-lysine coated cover slips, then sealed and stored at 4℃.

3.1.7 Cloning of PfAMPD into pGLUX plasmid

PfAMPD was tagged with GFP at C-terminal using pGLUX plasmid (plasmid image provided in the appendix) containing chloroquine resistance transporter promoter. The gene was amplified using primers ***ampd-gfp-fp-xho1 and ampd-gfp-rp-kpn1*** *(see appendix for sequences)* and digested using enzymes XhoI and KpnI. This was ligated to pGLUX plasmid, transformed to competent XL10 gold cells and grown at 30℃ for 24hrs. The clone was confirmed by standard protocols mentioned earlier.

3.2 Results and discussions

Dot blot and Western blot using anti-AMPD antibodies

Dot blot was performed to determine the optimum antibody titre [Figure 21]. Western blot was performed using pure protein and probed using anti-$(His)_6$ as well as anti-AMPD antibody for comparison purpose [Figure 22A]. Specificity of the antibody was also determined by probing it against Western blot [Figure 21B] done using whole cell lysates of *E.coli* (vector control and test).

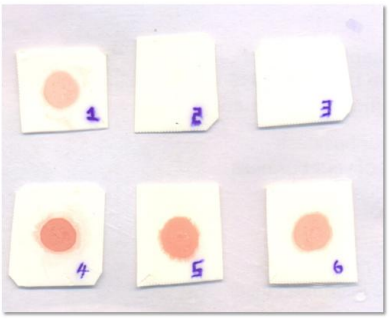

Figure 21.Determination of antibody titre by dot blot following methodology described in the text.

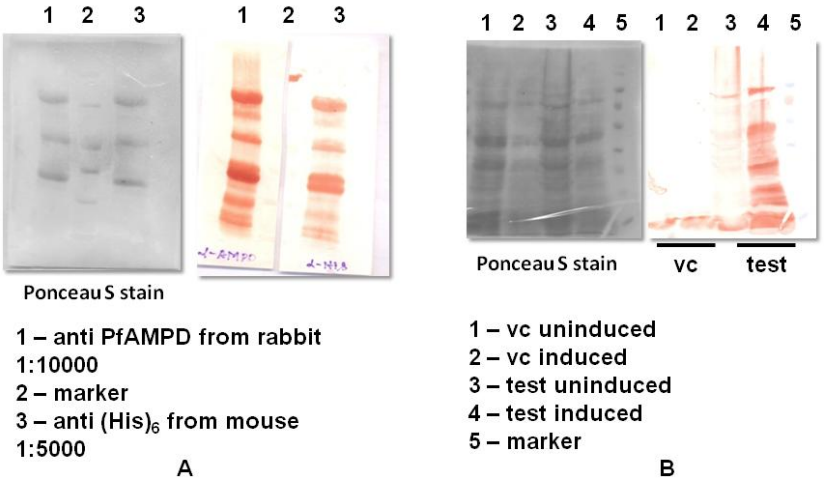

Figure 22.A) comparison of western blot profile of purified PfAMPD probed using anti-$(His)_6$ antibody from mice and anti-AMPD antisera from rabbit. B) Determination of specificity of the antibody by probing against whole cell lysates .Marker is as described earlier.

The antibody titre was found to be very high and the Western blot profile of anti-$(His)_6$ as well as anti-AMPD antibody was found to be similar. In fact the anti-AMPD antibody gave better signal than the commercial antibody. Also the antibody did not pick any protein from the vector control *E.coli* lysates, indicating that it is specific for PfAMPD only.

Western blot analysis of parasite lysate showed presence of a full length AMPD band of a faint intensity and a degradation band of high intensity. Bands were detected in both pellet and lysate supernatant fractions [Figure 23]. Non specific bands were observed in empty erythrocyte lane. Antibody concentration has to be decreased and the experiment has to be repeated. The presence of lower molecular weight band in the lane containing parasite lysate has to be further validated.

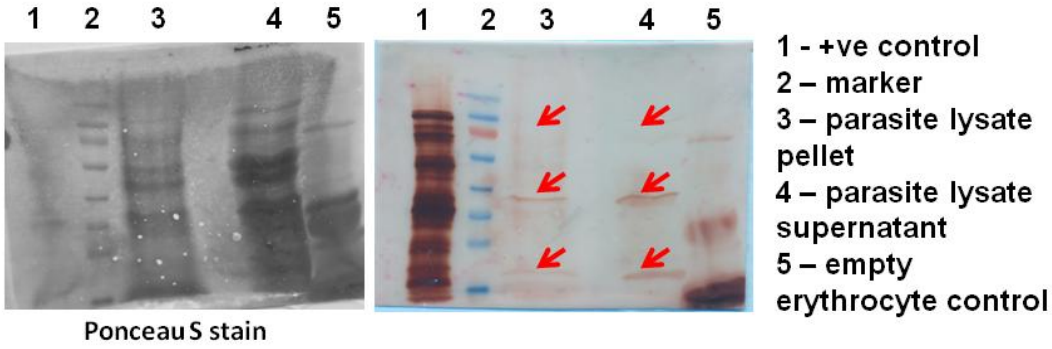

Figure 23.Western blot performed using erythrocytes and parasite lysate. Degradation band of PfAMPD was detected in both pellet and supernatant fractions. Faint full length band could also be seen. Arrows have been placed to indicate signals on the western.

Immunofluorescence

Parasites at late trophozoite to Schizont stage were harvested and immunofluorescence was performed. Antibody concentration and dilution was normalised across pre immune control and immune antibody. Secondary antibody was goat anti-rabbit which was conjugated to fluorophore, alexa488 (excitation 495nm and emission 519nm). Propidium iodide (excitation 535nm and emission 617nm) was used for nuclear staining. In pre immune control signal was not seen in most of the parasitized erythrocytes. But in few, punctate structures and faint background was observed [Figure 24A]. Whereas in the immune sera diffused cytosolic signal was seen in parasitized erythrocytes and not in empty erythrocytes [Figure 24B]. PfAMPD was seen to be localized in the parasite cytosol.

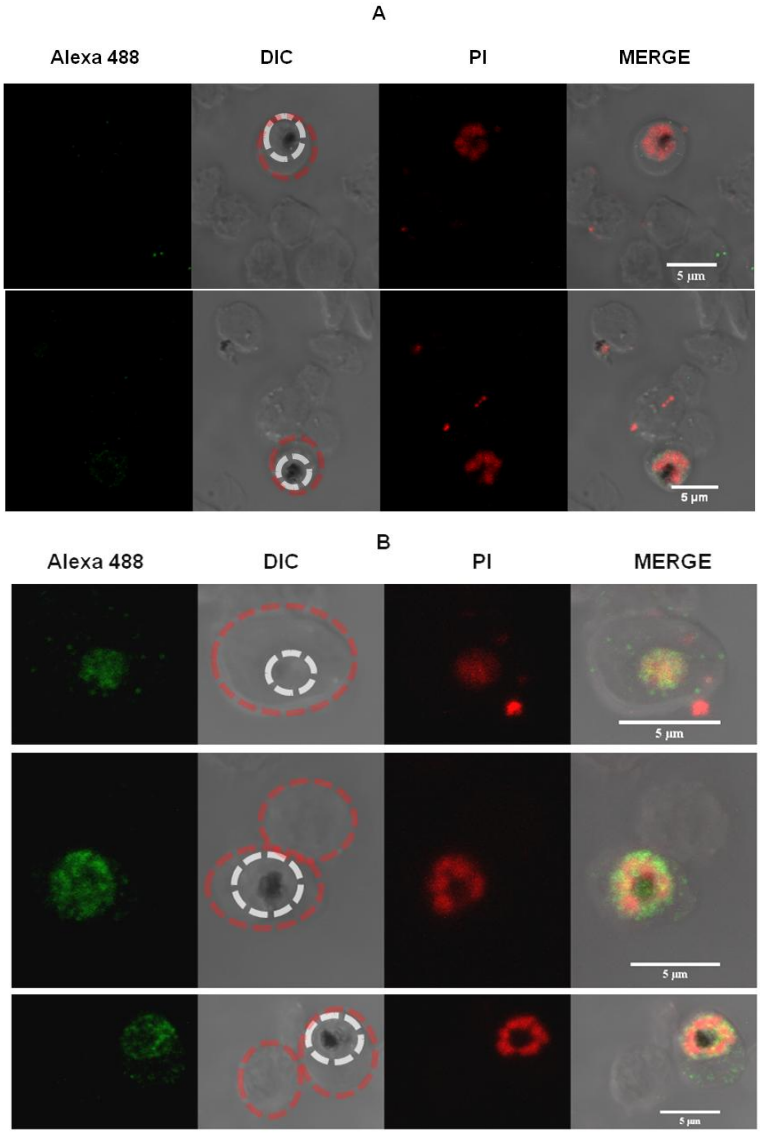

Figure 24.A) Parasite culture probed with pre immune antibody. B) Parasite culture probed with immune antibody. Red circle represents the erythrocyte boundary, whereas white circle represents parasite.

Punctuate structures seen in parasitized erythrocytes and also faint background in pre immune sera might be a true signal or an experimental artefact. To eliminate artefacts PfAMPD was tagged with GFP at C-terminal in pGLUX plasmid containing chloroquine resistance transporter promoter. The clone was confirmed by standard protocols Figure 25. This clone will be transfected to the parasite.

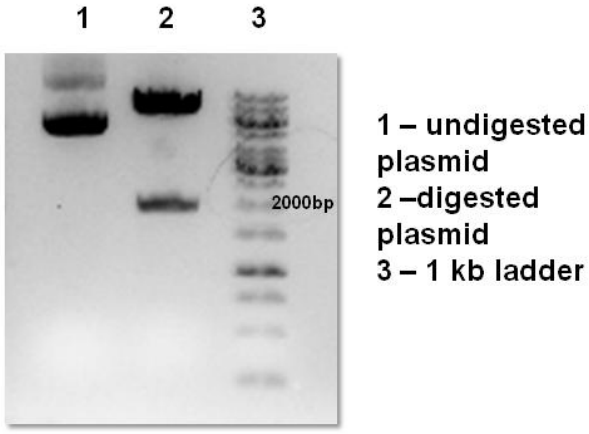

Figure 25.Clone confirmation of C –term GFP tagged PfAMPD by insert release.

Chapter 1	• Introduction
Chapter 2	• Expression of PfAMPD in *E. coli* and yeast
Chapter 3	• Localization studies in *P. falciparum*
Chapter 4	• **Complementation studies in AMPD knockout yeast strain**

Chapter 4 – Complementation studies in AMPD knockout yeast

Functionality of a protein can be determined by complementation experiments in heterologous systems like yeast, if homologous protein is present. Yeast has single AMP deaminase gene *AMD1* encoding an 810 amino acid protein AMPD. AMPD knockout yeast strain grows normally in regular growth media, but under metabolic stress, i.e. in the presence of adenine in the media, it shows a growth defect phenotype. This is because adenine from media gets taken up by the cells by nucleobase transporters and gets converted to AMP by APRT enzyme. Due to the absence of AMPD, AMP accumulates and inhibits the *de novo* pathway enzyme glutamine PRPP amidotransferase. This leads to drop in the production of IMP; a common metabolite which can feed in to AMP and GMP synthesis. Depleted GMP production leads to depleted GTP levels and thereby, perturbs protein biosynthesis. This manifests as a growth defect phenotype. This can be rescued by episomal expression of a functional AMPD from yeast itself or any other organism. Metabolic rescue of this phenotype can be done by adding hypoxanthine to the media which will form IMP upon phosphoribosylation by HGPRT or by adding aminoimidazole carboxamide ribonucleoside (AICAr) which will also form IMP via *de novo* pathway [Figure 26].

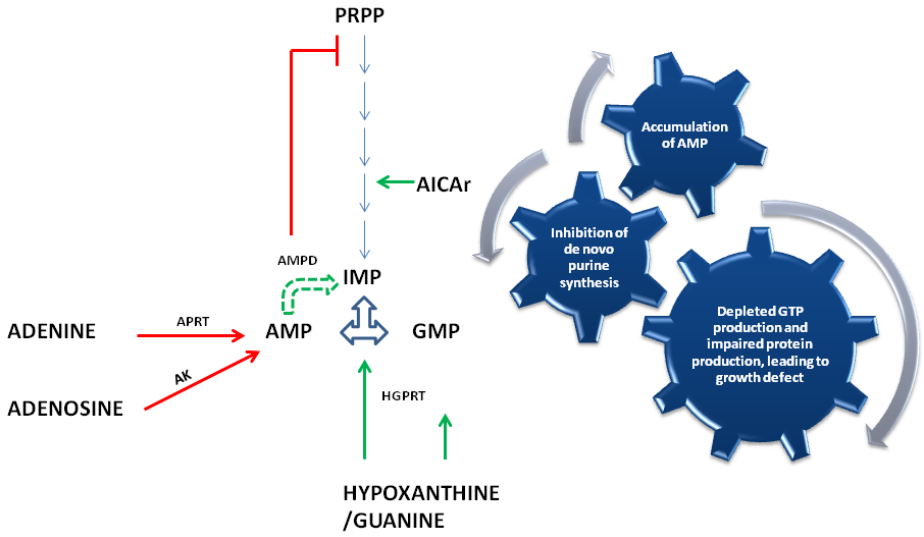

Figure 26.Schematic showing principle behind adenine toxicity in Δamd1 yeast strains. Red arrows are possible modes of establishment of toxicity and green arrows are the ways through which rescue can be achieved. Dotted green arrow indicates the mode of rescue by expression of functional AMPD (Akizu et al., 2013, Rebora et al.,

2001 and Marc et al. 2009). The interlocked gear represented on the right is to highlight the series of events that result from AMP accumulation. AMP accumulation leads to inhibition of de novo purine synthesis that in turn depletes GTP levels resulting in growth arrest.

4.1 Materials and methods

All chemicals and reagents and media were procured from Sigma Aldrich, USA; Fischer chemicals, USA. Primers for cloning were obtained from Sigma Aldrich, India. Media components were obtained from Himedia, Mumbai (media composition is given in the appendix). Restriction enzymes, Phusion polymerase, T4 DNA ligase were obtained from New England Biolabs and used according to manufacturer's instruction. Cloning strain XL-10 gold was from Novagen, India. Knockout yeast strain *Δamd1* (*MATα; his3Δ 1; leu2Δ 0; lys2Δ 0; ura3Δ 0; YML035c::kanMX4)* and plasmid pCM189 (see appendix for vector map) were obtained from EUROSCARF, Germany. Wild type yeast strain BY4742 and pYES2/CT plasmid were kind gifts from Dr. Ravi Manjithaya, MBGU, JNCASR and Prof. G. Padmanabhan, Dept. of Biochemistry, Indian Institute of Science, Bangalore. S-adenosyl methionine was a generous gift from Prof. Umesh Varshney's lab, Indian Institute of Science. Plasmid isolation and PCR purification kits were from Qiagen, Netherlands.

4.1.1 Cloning and transformation

Cloning of PfAMPD in pYES/2CT has been described in methods of chapter 2. Knockout yeast was transformed with pYES2/CT*Pf*AMPD i.e. plasmid containing PfAMPD gene under *Gal1* promoter. Empty plasmid was also transformed separately to serve as vector control. The transformants were selected on SD-uracil plates and screened by PCR as described earlier. Also, PfAMPD (test) and *Saccharomyces cerevisiae* AMPD (ScAMPD) (+ve control) were cloned into pCM189 using the primers ***pfampd cla1 fp, pfampd pst1 rp, yeastampd stu1fp and yeastampd pst1 rp*** (see appendix for primer sequence). Since the forward primers for cloning in pCM189 plasmid lacked the desired restriction sites, restriction digestion of

this end was done using appropriate enzymes and the overhang filled-in using Klenow enzyme. This was followed by digestion of the 3′ end using PstI. Similarly, the plasmid pCM189 was also digested by BamHI, filled-in and digested with PstI. The PCR product and the plasmid were ligated, transformed to XL-10 gold cells and incubated at 30℃ for 24hrs. Clones were confirmed and the knockout strain *Δamd1*was transformed with the plasmids, pCM189PfAMPD and pCM189ScAMPD. pCM189 plasmid was also transformed as control. Yeast transformants were confirmed by protocols described earlier.

4.1.2 Serial dilution and spotting assay

Single colonies from test and control plates were inoculated to 5mL SD-uracil liquid media (with glucose as carbon source, which will repress protein expression), grown overnight at 30 ℃. The cells were harvested and washed with sterile water twice and OD was determined at 600nm. Ten fold serial dilutions were made starting from 1OD/mL to 10^{-4} OD/mL. 3µL of culture from each dilution was spotted on SD-uracil plate (containing galactose as carbon source, which will induce protein expression) with and without adenine, allowed to dry and incubated at 30℃ for 48-72hrs. The plates were observed for cell growth and photographically documented. As control, plating was also done on glucose containing plates. In case of cells containing pCM189 plasmid and clones made in pCM189, spotting was done on glucose containing plates in the absence of doxycycline.

4.2 *Results and discussions*

Cloning of PfAMPD and yeast AMPD

The plasmid, pCM189 used for complementation has a tet O7 system, where gene expression is turned-off in the presence of doxicycline and induced in its absence. *Plasmodium* and yeast AMPD genes were cloned into pCM189 plasmid and the clones were confirmed by

restriction digestion using BamHI and PstI enzyme. Since both genes contained an internal BamHI site two bands are seen instead of one on the electropherogram [Figure 28].

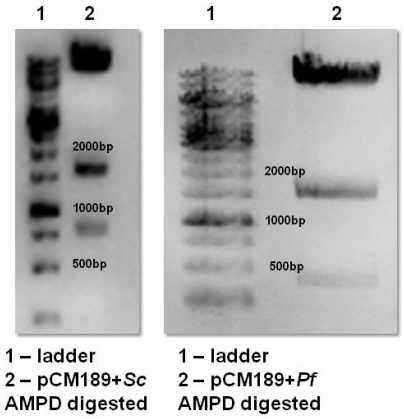

Figure 27.Clone confirmation of yeast (ScAMPD) and PfAMPD by restriction digestion and insert release. Samples loaded in different lanes are as mentioned.

Δamd1 strain confirmation and growth defect phenotype due to adenine toxicity

Confirmation of knockout strain was done by PCR. The schematic of PCR and the gel picture is as shown in Figure 28. Using upstream and downstream primers PCR was performed using genomic DNA of wild type and AMPD knockout yeast. Since the AMPD ORF is replaced in the knockout strain by G418 cassette a lower size band is obtained in this strain when compared with the wild type.

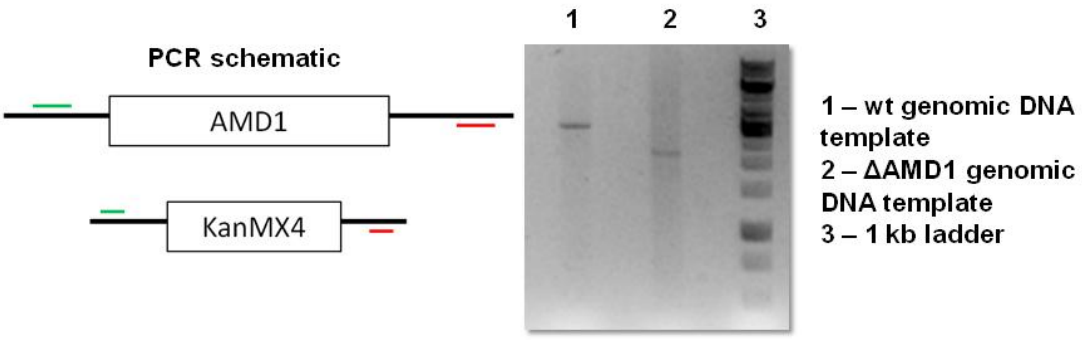

Figure 28.Yeast strain confirmation by PCR. Schematic is shown on the left panel and electropherogram of the PCR products is shown on right. Sample loaded in the lanes are as mentioned.

Serial dilution and spotting assay was done using wild type and *Δamd1*in the presence and absence of adenine in growth media to show growth defect phenotype. *Δamd1*strain shows growth defect phenotype in the presence of adenine where as wild type grows normally [Figure 29].

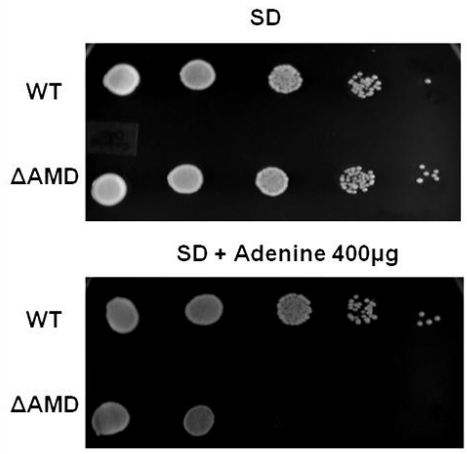

Figure 29.Phenotype of wild type and Δamd1 yeast strain in presence and absence of adenine in SD medium. Deletion of AMD1, the gene that codes for AMPD leads to growth inhibition in media supplemented with adenine.

Complementation assay

The *Δamd1* strain showing the growth defect phenotype was used for complementation assays. PfAMPD was cloned into pYES2/CT, followed by transformation of *Δamd1* using this construct and complementation assay was carried out by serial dilution and spotting. Control used was pYES2/CT alone. Surprisingly it was found that pYES2/CT alone could rescue the growth defect phenotype seen in the presence of adenine in *Δamd1* [Figure 30]. Therefore the question of whether PfAMPD complements ScAMPD deficiency is not answered.

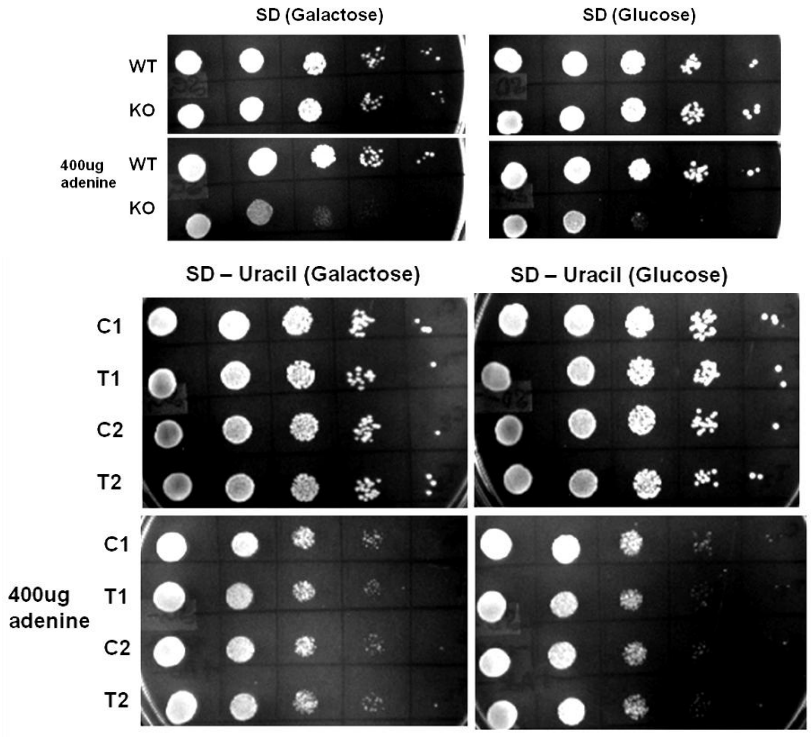

Figure 30.Complementation assay. Serial dilution assay was performed using WT – wild type, KO – knockout, C1 and C2 – vector control transformants, TI and T2 – transformants containing episomal PfAMPD. Growth

defect in Δamd1 strain (KO) is rescued by empty vector (C1 and C2) as well as plasmid containing PfAMPD (T1 and T2).

A second plasmid pCM189 was then used as a control. *Δamd1* was transformed with this plasmid and spotting assay was carried out comparing phenotype of pYES2/CT and pCM189 transformants. pYES2/CT transformant showed rescue of growth defect, whereas pCM189 did not show rescue, thereby behaving as expected [Figure 31]. The experiment had revealed an intriguing observation that the empty 2μ plasmid, pYES2/CT alone was able to rescue the growth defect phenotype.

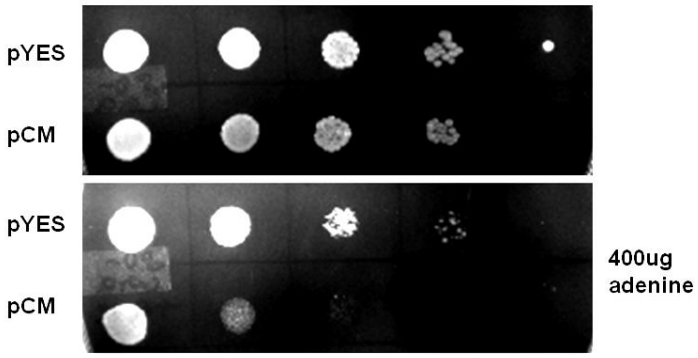

Figure 31.Serial dilution and spotting assay done using pCM189 plasmid transformant (pCM) and pYES2/CT plasmid transformant (pYES). The pYES2/CT plasmid transformant shows rescue of phenotype.

To explain this unexpected observation in pYES2/CT transformants, examination of the nature of both the plasmids was done. This led us to put forth a hypothesis based on metabolic perturbation involving OMP decarboxylase encoded by the *URA3* gene which is the marker in both plasmids.

The knockout strain *Δamd1* is auxotrophic for uracil while transformants carrying either pYES2/CT or pCM189 are not auxotrophic for uracil as the plasmids carry the gene *URA3* that codes for OMP decarboxylase (OMPD). The difference between pYES2/CT and pCM189 is their copy number: pCM189 is present in 1-2 copies per cell, while the copy number of pYES2/CT is 50-100 per cell. Though the promoters upstream of *URA3* are similar in both the plasmids, the variation in copy number could lead to elevated levels of the enzyme OMPD in cells transformed with pYES2/CT. OMPD catalyses the conversion of

OMP to UMP. Increase in OMPD levels would lead to rapid depletion of OMP a product of the reaction catalysed by OPRT. This in turn would lead to a higher flux of conversion of orotate to OMP, a reaction that utilises PRPP. It is possible that in cells expressing higher levels of OMPD, there is a lowering of PRPP levels and therefore this metabolite concentration becomes limiting and poorly available to APRT. Under such conditions the levels of AMP generated by the reaction of adenine with PRPP may not reach toxic levels and as a consequence adenine toxicity is not seen in cells carrying pYES2/CT [Figure 32]. Thus, this appears as an apparent rescue of the defective growth phenotype. The higher level of expression of OMPD in cells carrying pYES2/CT appears to phenocopy expression of functional AMPD. Similarly, yeast expressing defective GMP kinase was found to phenocopy HGPRT deficiency (*Leqoc et al., 2000*).

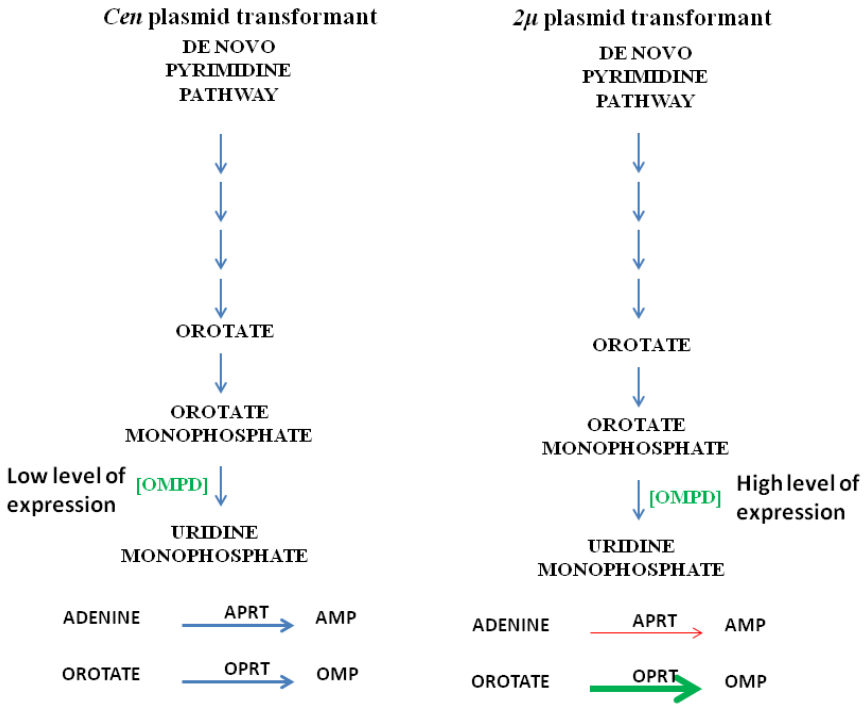

Figure 32.Schematic showing the possible mode of rescue from adenine toxicity in Δamd1 strain of yeast transformed with pYES2/CT. Increase in flux through the OPRT pathway consumes PRPP and thereby affects efficient conversion of adenine to AMP by APRT. This leads to insufficient levels of AMP accumulation failing to cause growth defect phenotype.

This hypothesis was put to test by altering the mode of toxicity. Adenosine can also form AMP via adenosine kinase pathway and unlike APRT this pathway is PRPP independent. Hence, irrespective of the type of plasmid used, whether pYES2/CT or pCM189 toxicity will be persistent. But due to the fact that yeast cells lack adenosine transporters adenosine could not be used, instead S-adenosyl methionine (SAM) a precursor of adenosine was used to induce toxicity which is independent of cellular PRPP levels. SAM is taken up by SAM permeases and then gets demethylated to give S-adenosyl homocysteine, which further gets hydrolysed to adenosine and homocysteine. Now this adenosine can get phosphorylated and induce toxicity in *Δamd1* strain by forming AMP. Serial dilution and spotting assays were done using both pYES2/CT plasmid transformant and pCM189 plasmid transformant in the presence and absence of SAM [Figure 33]. Now both the transformants showed growth defect and there was no difference between the two, thereby providing ample evidence justifying the hypothesis. Isolation and quantitation of metabolites from the various strains should confirm the above observations. This can also be further validated by episomal expression of OMPD gene in *Δamd1* strain.

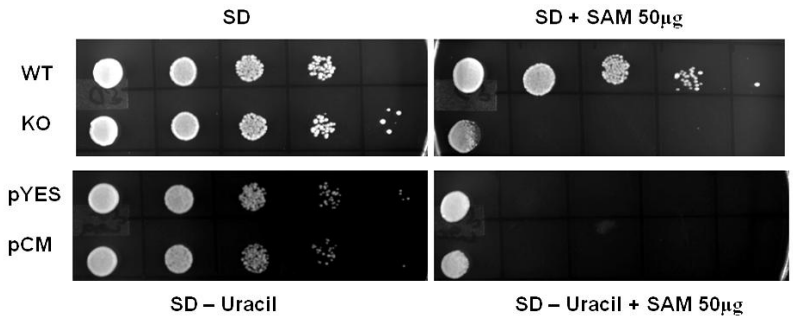

Figure 33.Phenotype of wild type, Δamd1 as well as Δamd1 transformed with pYES2/CT and pCM189 plasmids when grown on SAM containing plate. Transformant carrying either pYES2/CT or pCM189 showed similar phenotype unlike the different phenotypes seen on adenine containing plates,

Having established the fact that the inherent property of the pYES2/CT plasmid can possibly alter metabolic flux that utilizes PRPP in the transformants and rescue the growth defect phenotype, pCM189 was chosen as the plasmid to be used to perform functional complementation. Cloning was done as described in the methods, followed by

transformation of *Δamd1* using the constructs (PfAMPD and ScAMPD in pCM189). Serial dilution and spotting assay was done on SD-uracil plates with and without adenine [Figure 34]. Rescue of phenotype was seen in case of positive control only, but not in case of vector control and test. The experiment was also done on SAM containing plates and the results were similar.

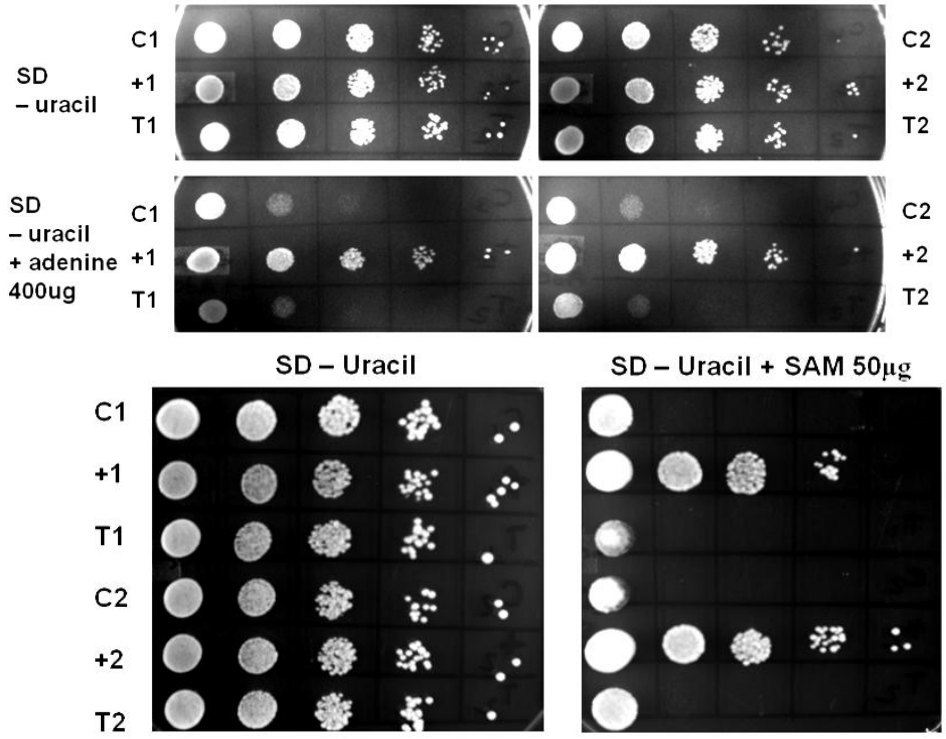

Figure 34.Complementation assay done using AMPD constructs made in pCM189. Cells containing pCM189PfAMPD (T1 and T2), do not show rescue of growth defect phenotype unlike cells containing pCm189ScAMPD (+1 and +2) which overcome the growth defect.

Conclusions and future plans

Expression in E. coli

It was found that in the bacterial expression system PfAMPD is expressed to a good extent, but suffered from proteolysis and went in to insoluble fraction. On the contrary, in yeast, the protein was soluble but expression was very low. The pattern of protein degradation (probed with anti-$(His)_6$ antibody) seen in the bacterial expression system suggested the presence a specific region susceptible to proteolysis. In the N-terminal $(His)_6$ -tagged construct, apart from full length band the major degradation band seen corresponded to approximately 53kDa and the major degradation band seen in case of C-terminal $(His)_6$ -tagged construct had molecular weight of approximately 37kDa.Though it could not be ascertained with great confidence, where exactly the protein is cleaved, a window of around 10kDa region was mapped that might contain the susceptible site [Figure 35].

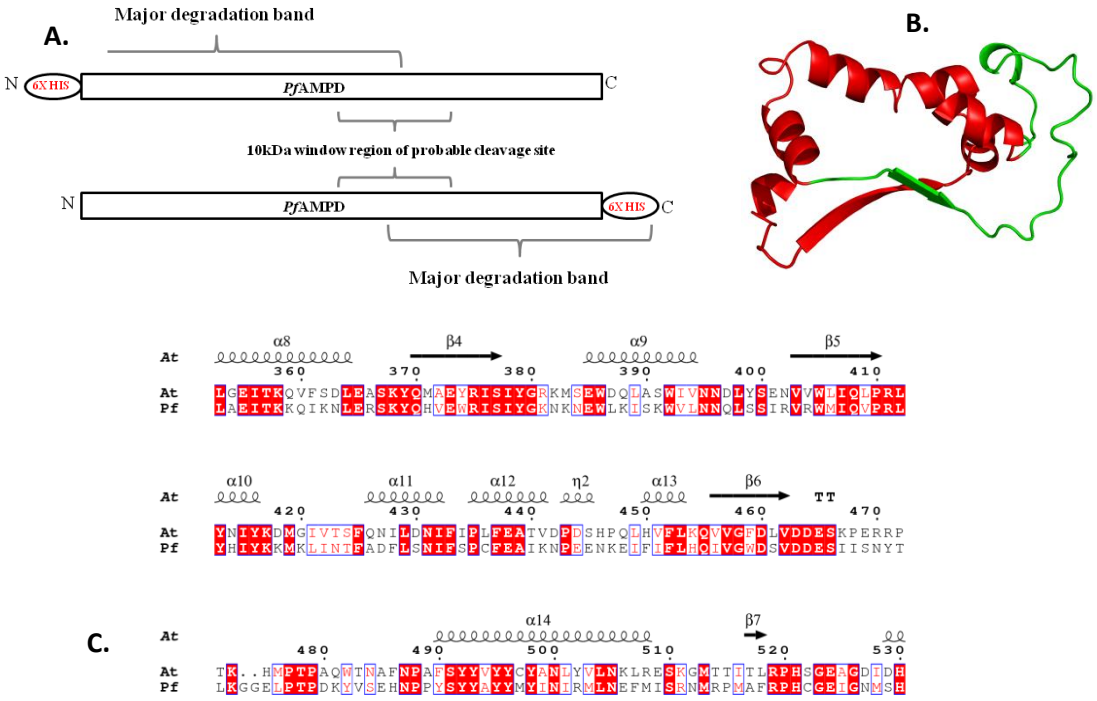

Figure 35.Schematic representation of the degradation pattern seen in the 6X $(His)_6$ -tagged PfAMPD and mapping of the 10kDa window region (amino acid 386 – 490) containing putative cleavage site. Panels B and C show an alignment and the structure, respectively of this 10kDa region. The structure of PfAMPD has been generated by homology modelling using AtAMPD as template. The region shown in green colour in the structure is a disordered segment that may be susceptible to proteolysis. This requires experimental validation

The exact cleavage point has to be identified and mutation or deletion at this region might result in obtaining a stable protein. This will be done by selectively enriching the N-terminal peptide of the full length and truncate proteins using reported methodologies (*Kleifeld et al., 2011*) followed by their identification using mass spectrometry.

Expression and complementation in yeast

Our experiments in wild type yeast show that expression levels of PfAMPD are low. In case of complementation studies in *Δamd1* yeast strain, the transformants containing PfAMPD failed to show rescue of growth defect phenotype. This could be due to different reasons. Low expression levels of PfAMPD could be one of the reasons. Expression check using *Δamd1* carrying pCM189PfAMPD was performed by Western blot and faint bands corresponding to full length protein and truncated forms were seen (data not shown). But when cells were grown in the presence of adenine, protein was not detected (data not shown). In this regard we first need to examine whether full length RNA is synthesised by RT-PCR followed by immunofluorescence microscopy for intra-cellular protein levels. Currently experiments using an endonuclease temperature sensitive mutant yeast strain, *rna15* (*LaCount et al., 2009),* which is capable of maintaining long AT rich mRNA in a stable manner, are also under way to obtain optimum expression of PfAMPD. Further, codon optimised synthetic gene of PfAMPD will be used to improve expression levels in the yeast system. Over- expression of tagged PfAMPD will also be carried out in the parasite itself, where folding and stability may be achieved as this is the native system. This has been exploited from some proteins of *P. falciparum* and *Toxoplasma gondii* such as Sir2 (silent information regulator), IMP dehydrogenase etc. (*Sullivan et al., 2005; Merrick and Duraisingh, 2007*).

Studies on P. falciparum

Stage specific parasite culture will be to be used to perform immunofluorescence to provide the complete picture regarding the localization of AMPD in different erythrocytic stages of *P. falciparum*. Further the culture will also be treated with appropriate reagents to select for only gametocytes (*Miao et al., 2013*). These gametocytes will be examined for localisation of AMPD by immunofluorescence. Further expression will also be examined in a stage specific manner by RT-PCR and Western blot. Also the plasmid containing GFP tagged PfAMPD that has been generated will be transfected to the parasites and examined for expression and localisation.

Essentiality of AMPD is not known in *P. falciparum*. A conditional knockout parasite of AMPD will be made by chromosomally tagging the gene with *E. coli* dihydrofolate degradation domain (DDD) (*Muralidharan et al., 2011).* The resultant fusion protein will be intact only in the presence of the ligand trimethoprim, as it stabilises the DDD. In the absence of the ligand the DDD loses stability and undergoes proteosomal degradation. Along with the tag AMPD also gets degraded and the parasite now behaves like a knockout. Lack of AMPD will perturb the adenylate energy charge (AEC) of the parasite and the consequences of this event on the parasite's viability and metabolism will be studied.

References

- *Akizu N., Cantagrel V., Schroth J., Cai N., Vaux K., Mccloskey D., Naviaux R. K., et al. (2013). AMPD2 Regulates GTP Synthesis and Is Mutated in a Potentially Treatable Neurodegenerative Brainstem Disorder. Cell, 154(3), 505–517.*

- *Ambrish Roy, Alper Kucukural, Yang Zhang,(2010). I-TASSER: a unified platform for automated protein structure and function prediction. Nature Protocols, vol 5, 725-738.*

- *Askari A., and Jr J. E. Franklin (1965). Effects of monovalent cations and ATP on erythrocyte AMP deaminase. BBA - Enzymology and Biological Oxidation, 110(1), 162–173.*

- *Astrid G. Chapman and Daniel E. Atkinson (1973), Stabilization of Adenylate Energy Charge by the Adenylate Deaminase Reaction. The Journal of Biological Chemistry, 248(10), 8309-8312.*

- *Cassera M. B., Hazleton, K. Z., Riegelhaupt P. M., Merino E. F., Luo M., Akabas M. H., and Schramm V. L. (2008). Erythrocytic Adenosine Monophosphate as an Alternative Purine Source in Plasmodium falciparum. The Journal of Biological Chemistry, 283(47), 32889–32899.*

- *Chae S., Fuller D., and Loomis W. F. (2002). Altered Cell-Type Proportioning in Dictyostelium Lacking Adenosine Monophosphate Deaminase. Developmental Biology, 194, 183–194.*

- *Chapman, A. G., Fall, L., and Atkinson, D. E. (1971). Adenylate Energy Charge in Escherichia coli During Growth and Starvation. The Journal of Bacteriology, 108(3), 1072–1086.*

- *Downie, M. J., Kirk, K., and Mamoun, C. Ben. (2008). Purine salvage pathways in the intraerythrocytic malaria parasite Plasmodium falciparum. Eukaryotic cell, 7(8), 1231–7.*

- *David J. Merkler, Anupam S. Wali, Taylor J. and Vern L. Shramm (1989). AMP Deaminase from Yeast. The Journal of Biological Chemistry 264(35), 21422–21430.*

- *Gari E. (1997). A Set of Vectors with a Tetracycline-Regulatable Promoter System for Modulated Gene Expression in Saccharomyces cerevisiae. Yeast Functional Analysis Reports, 848, 837–848.*

- *Haas A. L., and Sabina R. L. (2003). Expression , purification , and inhibition of in vitro proteolysis of human AMPD2 (isoform L) recombinant enzymes. Protein Expression and Purification, 27, 293–303.*

- *Han B. W., Bingman C. A., Mahnke D. K., Bannen R. M., Bednarek S. Y., Sabina R. L., and Phillips G. N. (2006). Membrane Association, Mechanism of Action, and Structure of Arabidopsis Embryonic Factor 1 (FAC1). The Journal of Biological Chemistry, 281(21), 14939–14947.*

- *Hellsten Y., Richter E. A., Kiens B., and Bangsbo J. (1999). AMP deamination and purine exchange in human skeletal muscle during and after intense exercise. Journal of Physiology, 909–920.*

- *Isackson P. J., Bujnicki H., Harding C. O., and Vladutiu G. D. (2005). Myoadenylate deaminase deficiency caused by alternative splicing due to a novel intronic mutation in the AMPD1 gene .Molecular Gnetics and Metabolism 86, 250–256.*

- *Jayaraman V., Bulusu V., and Balaram H. (2011). Crosstalk between purine nucleotide metabolism and mitochondrial pathways in Plasmodium falciparum. Current Science, 757–766.*

- *Kalsi K. K., Yuen A. H. Y., Rybakowska I. M., Johnson P. H., Slominska E., Birks E. J., Kaletha K., et al. (2003). Decreased cardiac activity of AMP deaminase in subjects with the AMPD 1 mutation — A potential mechanism of protection in heart failure. Cardiovascular Research, 59, 678–684.*

- *Kleifeld O., Doucet A., Prudova A., auf dem Keller U., Gioia M., Kizhakkedathu,J. N., & Overall C. M. (2011). Identifying and quantifying proteolytic events and the natural N terminome by terminal amine isotopic labeling of substrates. Nature protocols, 6(10), 1578–611.*

- *Lanaspa M. A., Cicerchi C., Garcia G., Li N., Roncal-jimenez C. A., Ishimoto T., Sa L. G., et al. (2012). Counteracting Roles of AMP Deaminase and AMP Kinase in the Development of Fatty Liver. Plos One, 7(11).*

- *Lecoq K., Konrad M., & Daignan-Fornier B. (2000). Yeast GMP kinase mutants constitutively express AMP biosynthesis genes by phenocopying a hypoxanthine-guanine phosphoribosyltransferase defect. Genetics, 156(3), 953–61.*

- *Li P., Ogino K., Hoshikawa Y., Morisaki H., Toyama K., and Morisaki T. (2013). AMP deaminase 3 plays a critical role in remote reperfusion lung injury. Biochemical and Biophysical Research Communications, 434(1), 131–136.*

- *Lowenstein, J. M. (1972). Ammonia Production in Muscle and Other tissues: The Purine Nucleotide Cycle. Physiological Reviews, 52(2), 382–414.*

- *Mary T. Bausch-Jurken and Richard L. Sabina (1995). Divergent N-Terminal Regions in AMP Deaminase and Isoform-Specific Catalytic Properties of the Enzyme. Archives of Biochemistry and Biophysics, 321 (2), 373-380.*

- *Martini D., Ranieri-raggi M., Sabbatini A. R. M., Moir A. J. G., Polizzi E., Mangani S., and Raggi A. (2007). Characterization of the metallocenter of rabbit skeletal muscle AMP deaminase. A new model for substrate interactions at a dinuclear cocatalytic Zn site. Biochimica et Biophysica Acta, 1774, 1508–1518.*

- *Marotta R., Parry B. R., and Shain D. H. (2009). Divergence of AMP Deaminase in the Ice Worm Mesenchytraeus solifugus. International Journal of Evolutionary Biology.*

- *Marko Lõoke, Kersti Kristjuhan, and Arnold Kristjuhan (2011). Extraction of Genomic DNA from Yeasts for PCR. Biotechniques 50(5), 325–328.*

- *Marquetant R., Sabina R. L., and Holmes E. W., (1989). Identification of a Noncatalytic Domain in AMP Deaminase That Influences Binding to Myosin. Biochemistry, 43, 8744–8749.*

- *Merklers J., and Schramm L. (1990). Catalytic and Regulatory Site Composition by Comparative Binding and Rate Studies. The Journal of Biological Chemistry, 265(8), 4420–4426.*

- *Merkler D. J., and Schramm V. L. (1993). Catalytic Mechanism of Yeast Adenosine 5'-Monophosphate Deaminase. Zinc Content, Substrate Specificity, pH Studies, and Solvent Isotope Effects. Biochemistry,32,5792–5799.*

- *Merrick, C. J., & Duraisingh, M. T. (2007). Plasmodium falciparum Sir2: an unusual sirtuin with dual histone deacetylase and ADP-ribosyltransferase activity. Eukaryotic cell, 6(11), 2081–91.*

- *Meyer S. L., Kvalnes-krick K. L., and Schramm V. L. (1989). Characterization of AMD, the AMP Deaminase Gene in Yeast. Production of amd Strain , Cloning , Nucleotide Sequence , and Properties of the Protein. Biochemistry, 1090, 8734–8743.*

- *Miao, J., Wang, Z., Liu, M., Parker, D., Li, X., Chen, X., & Cui, L. (2013). Plasmodium falciparum: generation of pure gametocyte culture by heparin treatment. Experimental parasitology, 135(3), 541–5.*

- *Morisaki T., Gross M., Morisaki H., Pongratz D., Zollnert N., and Holmes E. W. (1992). Molecular basis of AMP deaminase deficiency in skeletal muscle. PNAS. 89, 6457–6461.*

- *Murakamiij, K. (1985). AMP Deaminase Reaction as a Control System of Glycolysis in Yeast. The Journal of Biological Chemistry, (6), 4729–4732.*

- *Muralidharan, V., Oksman, A., Iwamoto, M., Wandless, T. J., & Goldberg, D. E. (2011). Asparagine repeat function in a Plasmodium falciparum protein assessed via a regulatable fluorescent affinity tag. PNAS, 108(11), 4411-4416.*

- *Nam S., Park H., and Kim H. (2005). Evolutionary Relationship and Application of a Superfamily of Cyclic Amidohydrolase Enzymes. The Chemical Record, 5, 298–307.*

- *Oa H. T., Sabina R. L., Paul A., Ferl R. J., Laber B., Lindell S. D., Hoechst W., et al. (2007). Adenine Nucleotide Pool Perturbation Is a Metabolic Trigger for AMP Deaminase Inhibitor-Based Herbicide Toxicity. Plant Physiology, 143, 1752–1760.*

- *Ouyang, J., Parakhia, R. A., and Ochs, R. S. (2011). Metformin Activates AMP Kinase through Inhibition of AMP. The Journal of Biological Chemistry,286, 1-11.*

- *Rébora K., Desmoucelles C., Borne F., Pinson B., Daignan-fornier B., and Desmoucelles C. (2001). Yeast AMP Pathway Genes Respond to Adenine through Regulated Synthesis of a Metabolic Intermediate Yeast AMP Pathway Genes Respond to Adenine through Regulated Synthesis of a Metabolic Intermediate. Molecular and Cellular Biology, 7901-7912.*

- *R Daniel Gietz and Robert H Schiestl (2007). High-efficiency yeast transformation using the LiAc/SS carrier DNA/PEG method. Nature protocol, 2(1), 31-34.*

- *Ricardo Martí Arbona (2006). Mechanistic characterization of members of the Amidohydrolase superfamily. (Ph.D thesis).*

- *Romanos M. A., Scorer C. A., and Clare J. J. (1992). Foreign Gene Expression in Yeast : a Review. Yeast, 8, 423–488.*

- *Roth E. J., Ogasawara N., Schulman S., and Cells R. (2013). The deamination of adenosine and adenosine monophosphate in Plasmodium falciparum-infected human erythrocytes: in vitro use of 2'deoxycoformycin and AMP deaminase-deficient red cells. The Journal of Molecular Biology, 1121–1125.*

- *Sabina R. L., Swain J. L., Olanow C. W., Bradley W. G., Fishbein W. N., Dimauro S., and Holmes E. W. (1984). Myoadenylate Deaminase Deficiency Functional and Metabolic Abnormalities Associated with Disruption of the Purine Nucleotide Cycle. Journal of Clinical Investigations, 73, 720-730.*

- *Saint-marc, Benoıˆt Pinson, Fanny Coulpier, Laurent Jourdren, Olesia Lisova and Bertrand D. Fournier, (2009). Phenotypic Consequences of Purine Nucleotide Imbalance in Saccharomyces cerevisiae. Genetics, 183, 529-538.*

- *Sullivan, W. J., Dixon, S. E., Li, C., Striepen, B., & Queener, S. F. (2005). IMP Dehydrogenase from the Protozoan Parasite Toxoplasma gondii, 49(6), 2172–2179.*

- *Xu J., Zhang H., Xie C., Xue H., Dijkhuis P., Liu C., (2005). EMBRYONIC FACTOR 1 encodes an AMP deaminase and is essential for the zygote to embryo transition in Arabidopsis. The Plant Journal, 42, 743–756.*

- *Yang Zhang (2008). I-TASSER server for protein 3D structure prediction. BMC Bioinformatics, 9, 40.*

Appendix

List of primers

OLIGO NAME	SEQUENCE	T_M	PURPOSE
pfampd-fp_ecori	TTTCCGGAATTCACGGTTACCT AATAAAAATGATGGTC	68	Cloning N-$(His)_6$ tag
pfampd-rp_hindiii	ATACCCAAGCTTTTAATTGTTT GATGAATAGCTAGCTAGTCG	68	Cloning N-$(His)_6$ tag
ampda.int. fwd.1	ATGAAGGACCTTCAAGCAG	59	Sequencing
ampda.int.rev.1	TTGAACGGGTTTTTATCAATAT G	61	Sequencing
δ59ampda ecori fp	TTTCCGGAATTCAACTTTAACG TCCACGGGG	68	N-deletion cloning
δ94ampda ecori fp	TTTCCGGAATTCAATCGACACT TGCCTTGTAGAAAG	68	N-deletion cloning
δ178ampda ecori fp	TTTCCGGAATTCAGCAGAAGAT TATTTATCTAGCATACAAGAAA TTATG	68	N-deletion cloning
ampd-gfp-fp-xho1	AAAGC CTCGAG ATGCGGTTACCTAATAAAAATG ATGG	65	C-gfp tag
ampd-gfp-rp-kpn1	ACACGG GGTACC ATTGTTTGATGAATAGCTAGCT AGTC	65	C-gfp tag
ampd c term-fp - nco1	AACTTG CCATGG CA CGGTTACCTAATAAAAATGATG GTC	65	Cloning C-$(His)_6$ tag
ampd c term-rp - xho1	ATACCG CTCGAG ATTGTTTGATGAATAGCTAGCT AGTCG	65	Cloning C-$(His)_6$ tag
ampd ol-ir	GAGGCCTGAATGCCATTGGTCT CATATTTCTAC	65	Overlap to remove Nco1
ampd ol-if	GTAGAAATATGAGACCAATGG CATTCAGGCCTC	65	Overlap to remove Nco1
new irev ampda	CAAGGCAAGTGTCGATATCTTG	63	Sequencing AMPDA in pGLUX
pyes ampd fp kpn1	ATCGGGGTACCATGTCTCGGTT ACCTAATAAAAATGATGGTCAT AAAACTG	66	Cloning in pYES2/CT
pyes ampd rp xba1	GGCTAGTCTAGATCACTTTGTT AGCAGCCGGATCTCAGTG	66	Cloning in pYES2/CT
dscampd c fp	AACTTTATTTTTAGGGCACGTG G	60	Confirmation of AMPD gene in yeast
dscampd c rp	ATTCGAGGTAAAAACTTCAACA GC	60	Confirmation of AMPD gene in yeast
yeastampd stu1fp	TATTGAAGGCCTATGGACAATC AGGCTACACAGAG	65	Cloning of yeast AMPD for complementation
yeastampd pst1 rp	ATAACTGCAGTCACTTTTCTTC AATGGTTCTCTTG	65	Cloning of yeast AMPD for complementation
pfampd cla1 fp	AACCATCGATATGCGGTTACCT AATAAAAATGATGGTC	65	Cloning of *Pf*AMPD for complementation
pfampd pst1 rp	GATGAACTGCAGTTAATTGTTT GATGAATAGCTAGCTAG	65	Cloning of *Pf*AMPD for complementation

Plasmid Maps

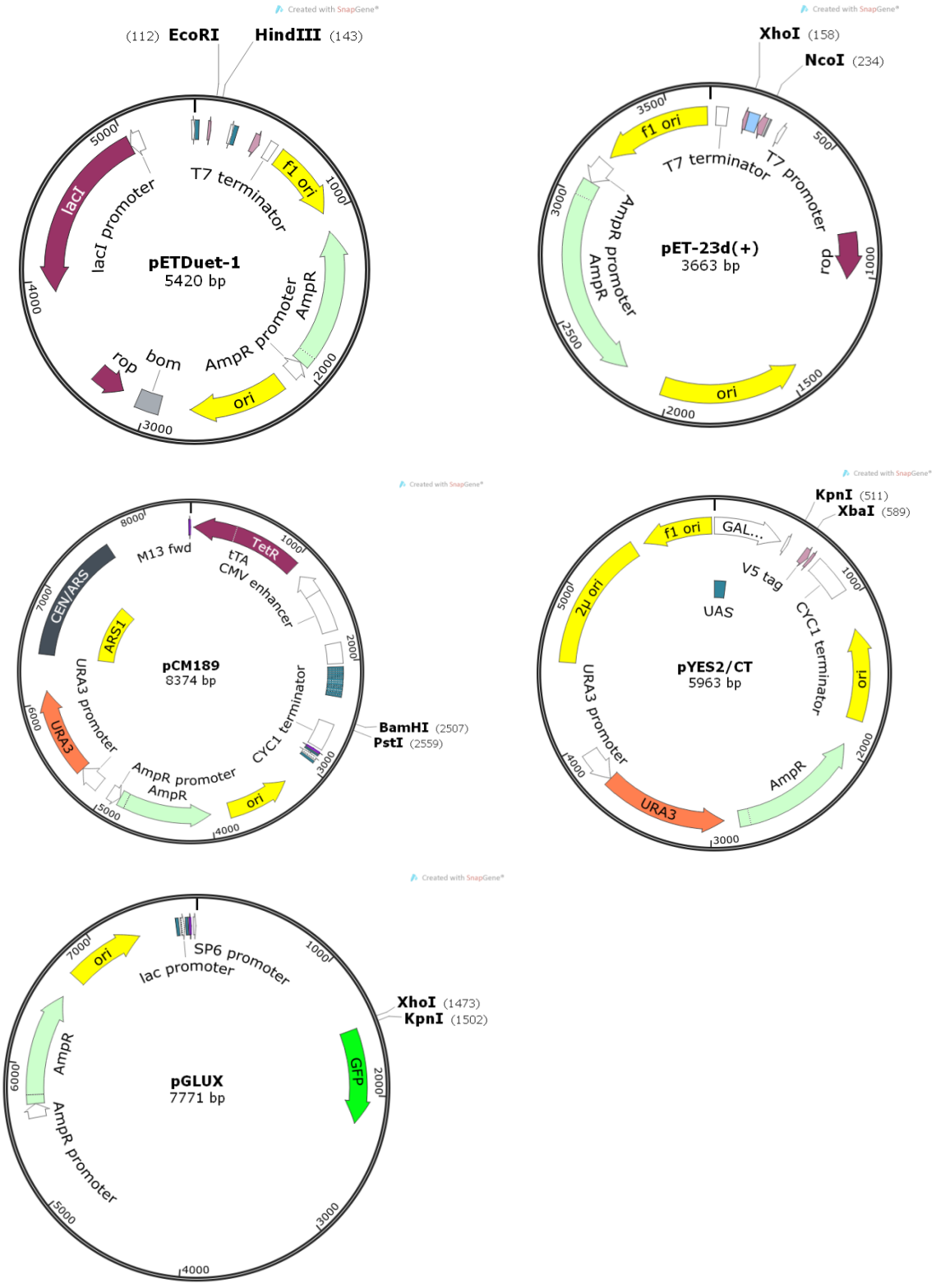

Figure 36.Different plasmids used for cloning. The restriction sites used for cloning are highlighted.

Yeast media composition

- YPD (100mL): Yeast extract – 1g, Peptone – 2g, Dextrose – 2g and Agar – 2g

Sugar, nitrogen base and amino acid stocks and working concentrations:

- Glucose/ Galactose: 20%; working 2%
- Yeast nitrogen Base without amino acids: 3.4% working 0.17%
- Histidine – 2% - stored in al foil in fridge (filter sterilize). Working 0.2 mL stock solution /200mL
- Leucine – 1% - stored in fridge (filter sterilize). Working 1.2mL stock solution /200mL
- Methionine – 2% - stored in fridge (filter sterilize). Working 0.2mL stock solution /200mL
- Uracil – 0.2% made in 1% sodium carbonate, stored at room temperature (filter sterilize). Working 2mL stock solution /200mL
- Lysine – 1.5% stored in fridge (filter sterilize). Working 0.4 mL stock solution /200mL
- Adenine – 20mg/mL in 1M HCl (working 400µg/25mL by spread plate technique)
- G418 50mg/mL stock (working 200 µg/mL)